Current Science International
Volume: 13 | Issue: 01| Jan. - March| 2024

EISSN:2706-7920 ISSN: 2077-4435
DOI: 10.36632/csi/2024.13.1.5
Journal homepage: www.curresweb.com
Pages: 43-74

The Possible Antihyperglycemic Effects of Zinc Oxide Nanoparticles On Diabetes Induced by Streptozotocin in Male Rats

Madiha M. Al Sulimani[1], Salim M. El Hamidy[1,2] and Abdulkader M. Shaikh Omar[1,2]

[1]Department of Biological Sciences, Faculty of Science, King Abdulaziz University, Jeddah, Saudi Arabia.
[2]Princess Dr. Najla Bint Saud Al-Saud Center for Excellence Research in Biotechnology, King Abdulaziz University, Jeddah, Saudi Arabia

Received: 20 Nov. 2023 **Accepted:** 21 Dec. 2023 **Published:** 15 Jan. 2024

ABSTRACT

Introduction: Zinc oxide nanoparticle therapy, is a possible treatment for a variety of diseases. Our objective was to investigate the therapeutic potential of ZnO NPs in correcting the histological and functional abnormalities in the liver and pancreas in a rat model of streptozotocin-induced diabetes. This study evaluated the safety and possible antidiabetic advantages of zinc oxide nanoparticles. **Methodology:** Seventy five mature male albino rats weighing between 180 and 200 grams were utilized. Following a week of acclimatization, the rats were split into five groups at random. Control group: didn't receive any medical attention, Diabetic group: received 45 mg/kg of streptozotocin intraperitoneally as a single dose, Diabetic and Zinc oxide nanoparticles group: a single oral dosage of 10 mg/kg ZnO NPs in suspension each day, Diabetic and chitosan group: a single oral dosage of 150 mg/kg chitosan each day and Diabetic, chitosan, and Zinc oxide nanoparticles group, an oral dosage of 150 mg/kg chitosan + 10 mg/kg ZnO NPs in suspension each day. After 6 weeks, blood samples were collected until use and Organs were rapidly removed after blood was drawn for biochemical analysis and histopathological studies. Further, obtained ZnO NPs characterized by SEM, EDS, TEM and XRD, and TEM analysis **Results:** A combination of histological investigation and blood biochemical research was employed to confirm the effectiveness of encapsulating chitosan with ZnO nanoparticles in the management of diabetes mellitus in rats. Oral administration of zinc oxide nanoparticles resulted in significant antidiabetic effects that is, improved glucose tolerance, higher serum insulin, reduced blood glucose. Nanoparticles were systemically absorbed resulting in elevated zinc levels in the liver and pancreas. **Conclusion:** This demonstrates the potential for controlling diabetes and the therapeutic use of ZnO NPs and chitosan as a safe anti-diabetic medication.

Keywords: Diabetes Mellitus, ZnO NPs, chitosan, liver function, oxidative stress

1. Introduction

Diabetes mellitus (DM) is a metabolic condition brought on by a reduction in insulin and/or insulin secretion in the body (Padhi *et al*., 2020).

Hyperglycemia, or elevated blood sugar, is a sign of diabetes, a long-term metabolic illness mostly caused by insufficient insulin production and/or activity of the insulin hormone in pancreatic beta cells (Rodrigues *et al.,* 2020). Diabetes is seen as a health risk in both developed and underdeveloped countries. The effects of this disease may include retinal, neuropathy, nephropathy, cardiovascular problems, and hepatopathy, to name a few degenerative and irreversible conditions.

The small intestine, liver, and spleen surround the organ known as the pancreas, which is situated in the upper left section of the abdomen beyond the stomach. Digestive enzymes are made by the pancreas. Additionally, it produces the hormone insulin (beta cells are the cells that produce insulin), which helps regulate blood sugar levels by facilitating the transfer of glucose from the blood

Corresponding Author: Madiha M. Al Sulimani, Department of Biological Sciences, Faculty of Science, King Abdulaziz University, Jeddah, Saudi Arabia.
E-mail: bluesky_1406@hotmail.com.

to adjacent cells. The pancreas is encircled by numerous main blood arteries that supply blood to the organ and other abdominal organs, including the celiac axis, portal vein, superior mesenteric artery, and superior mesenteric vein. Insulin resistance, or the pancreas producing little or no insulin at all, is the cause of diabetes mellitus. This is known as hyperglycemia because cells are no longer able to absorb glucose from the blood. As a result, blood glucose levels rise. The majority of diabetic symptoms and issues are brought on by hyperglycemia (Alizadeh *et al.,* 2020).

Non-alcoholic fatty liver disease (NAFLD) and type 2 diabetes mellitus (T2DM) are two very frequent metabolic liver illnesses. The precise cause of the strong correlation between T2DM and NAFLD, despite an increasing amount of epidemiological studies pointing to this connection, is still unknown. The body's metabolism of nutrients and energy is centered in the liver. Here, we have demonstrated via several studies the pathophysiology linking T2DM and NAFLD, as well as the decrease in T2DM progression after NALFD improvement in a cohort study. We proposed that the development and management of NAFLD medications is urgently needed and could lead to new avenues for type 2 diabetes treatment (Xiong and Li, 2023).

Information about the start of hepatic decompensation in patients with non-alcoholic fatty liver disease (NAFLD) and type 2 diabetes is lacking (Huang *et al.,* 2023).

Natural source nutritional supplements are becoming more and more popular, and they may be a better option than store-bought anti-diabetic medications. Priyanka *et al.* (2022) a new study focused on the vital processes and advantages in lowering blood sugar that are mostly linked to chitosan derivatives while treating hyperglycemic illnesses. Chitosans and its derivatives have been shown in studies to have anti-diabetic effects both in vivo and in vitro. These effects are mediated through glucose absorption, insulin resistance, and lipid metabolism.

Minimal molecular weight One of the chitosan derivatives that has been demonstrated to maintain its original pharmacological qualities while exhibiting enhanced biocompatibility, bioactivity, biodegradability, and non-toxicity is chitosan. These characteristics include the capacity to stimulate erythrocyte aggregation, platelet activation, and other chitosan-like pathways (Wang *et al.,* 2020).

Studies have shown a connection between high blood sugar and hepatocellular carcinoma, cirrhosis, nonalcoholic fatty liver disease, glycogen deposition, fibrosis, and significant elevations in liver enzymes. Furthermore, an improper accumulation of fat in the liver may cause major metabolic issues (Mohamed *et al.,* 2016).

Oxidative stress is thought to play a key role in the pathogeneses of type 2 diabetes and the emergence of diabetic complications (Kliszczewska, 2020).

Four main pathways can be used to explain the difficulties associated with diabetic mellitus: the hexamine pathway, the polyol pathway, the activation of protein kinase C, the development of advanced glycosylation end products (AGE), and the production of reactive oxygen species (ROS), which is induced by hyperglycemia (Tabatabaie-Malazy *et al.,* 2017).

Over the years, Inflammation and oxidative stress have been identified as major factors in the onset and course of diabetes treatment and management; the first of these studies was published in 2018 (Duru *et al.,* 2018).

The two primary mechanisms associated with the formation of diabetes-related liver disorders are the generation of reactive oxygen species (ROS) and oxidative stress caused by hyperglycemia. Oxidative stress and ROS production brought on by hyperglycemia enhance the generation of nitric oxide (NO) in diabetic liver injury. Lipid peroxidation and protein nitration, which are both brought on by NO's interaction with ROS, promote diabetes-related tissue damage (Oltulu *et al.*, 2019). The liver is one of the organs most impacted by oxidative stress caused by elevated blood sugar levels, as it is essential for regulating glucose metabolism (Gjorgjieva *et al.*, 2019).

Mohamed *et al.* (2016) state that increased levels of ROS and/or reactive oxygen species, such as hydrogen peroxide, superoxide, hydroxyl radicals, and singlet oxygen, as well as liver tissue necrosis, can result from hyperglycemia and oxidative stress.

In recent years, a wide variety of biomedical applications, including the monitoring, diagnosis, repair, and therapy of human biological systems, have shown significant promise for the use of nanotechnology and smart nanostructures. Due to their numerous biological activities, which can aid in the treatment of inflammation and diabetes problems, a number of nanoparticles are currently

utilized as alternative therapies (Abdulmalek and Balbaa, 2019). One may characterize the application of nanoparticles as a diverse field for insulin administration and glucose testing (Naser *et al.*, 2021).

Zinc is the trace element that is most abundant, second only to iron. It has immunomodulatory and antioxidant qualities and plays crucial roles in the emergence of several diseases, including dermatoses (Hawrysz and Woźniacka., 2023).

Well-known metal oxide nanoparticles with numerous uses in the fields of chemistry, medicine, and cosmetics are zinc oxide nanoparticles. Nonetheless, certain publications have also mentioned its toxicity, including toxicity to the liver, lungs, nerves, and immune system. (Keerthana and Kumar, 2020).

Numerous scholarly articles have proposed that ZnO NPs exposure triggers autophagy in immunological cells, renal tissue, gastrointestinal tract cells, and healthy skin cells (Hu *et al.*, 2019).

ZnO NPs are safe, biodegradable biopolymers that are frequently employed in the biomedical sectors for antidiabetic, antibacterial, anticancer, antifungal, drug delivery, and anti-inflammatory properties (Miao *et al.*, 2017; Kamal *et al.,* 2022).

Chitosan is a sugar derived from the external skeleton of shellfish, such as shrimp, crab, and lobster. It is utilized in the production of drugs and as medicine (Zhou *et al.,* 2017).

Because of their unique biological properties, which include being biocompatible, biodegradable, and generally nontoxic in the body in addition to their diverse biological activities (antimicrobial, antioxidant, and anti-inflammatory), they are widely used in biomedical and pharmaceutical fields, such as drug delivery, artificial skin, wound dressing, and biofilms (Guo *et al.,* 2020; Guan and Feng, 2022).

Chitosan is considered a highly biocompatible biopolymer with a wide range of applications due to its biodegradability, bioadhesivity, and bioactivity. Therefore, chitosan is a promising biopolymer with a wide range of prospective applications in the biomedical field, such as tissue engineering, wound healing, skin, bone, and kidney, nerve, and liver prosthetics. This biopolymer is also employed in the trapping of both organic molecules and pigments, as well as the selective separation of binary combinations. Moreover, chitosan can be used as a catalyst or as an initial molecule to produce goods with a large added value (Carmen *et al.,* 2020).

Chitosan is one of the many biopolymers found in nature, but it has drawn interest because of its innate antibacterial qualities (Ładniak *et al.,* 2022). Furthermore, Chitosan is a biodegradable, non-toxic polymer with high biocompatibility, low immunological response (Dimassi *et al.,* 2018), mucoadhesive (Ways *et al.,* 2018; Hasnain and Nayak, 2022), and absorption-promoting qualities. Chitosan is frequently employed in drug delivery systems (DDS) with enhanced biodistribution, higher specificity and sensitivity, and less pharmacological toxicity due to its advantageous qualities (Elkomy *et al.,* 2022; Cao *et al.,* 2022).

The goal of the current study is to effectively reduce the risk of complications from diabetes mellitus and enhance the therapeutic drug's delivery system by utilizing nanotechnology, specifically nanozinc oxide. This will help to overcome the serious side effects of therapy and the shortcomings of the previous therapeutic approaches. Numerous important medication delivery issues can be resolved by using nano zinc oxide.

2. Methodology

2.1. Materials

2.1.1. Chemicals

- Streptozotocin (STZ) and chitosan were bought from Sigma-Aldrich (Steinheim, Germany) as powder with a purity of approximately 95% and CAS number 18883-66-4.
- zinc oxide nanoparticles (ZnO NPs) from US Research Nanomaterials, Inc. in Houston, Texas (CAS No. 1314-13-2).
- Chitosan, low molecular weight (448869, Sigma-Aldrich, USA).

2.2. Methods

2.2.1. Structural Characterization:

FESEM, HRTEM, EDS, and XRD were used to characterize the ZnO NPs, chitosan, and ZnO NPs with chitosan in order to investigate their structural characteristics, surface morphology, and elemental composition analysis, respectively.

2.2.2. Constructing the STZ Solution and Inducing the DM

Before being used, STZ was dissolved in a pH 4.5, 10 mM sodium citrate buffer, and the isotonicity was adjusted by adding an appropriate volume of 0.25 M sodium chloride solution (Bennett and Pegg, 1981). After an overnight fast, a single intraperitoneal (IP) injection of a newly made streptozotocin solution at a concentration of 45 mg/kg body weight was used to induce diabetes in the experimental animals (Zafar *et al.,* 2009). The normal control rats (NCR) were provided with water exclusively. Following injection, the test rats were put back in their cages with unrestricted access to food and drink. Over the course of three days, DM was allowed to develop and stabilize in these rats who were receiving STZ. These rats were used to identify DM based on abstaining blood glucose stages. Rats with blood glucose levels greater than 300 mg/dL were classified as model rats with diabetes.

2.2.3. Configuring the suspension of ZnONP

ZnO nanoparticles (dispersions of 10–30 nm) were combined with 10 mg/ml of distilled water, and using an ultrasonic cleaner sonicator (Branson Ultrasonic Corporation, Danbury, Connecticut, USA), the combination was sonicated at ambient temperature for 30 minutes at 230 V. The suspension was immediately shaken on a vortex agitator prior to administration.

2.2.4. preparing the suspension of chitosan

An ultrasonic cleaner sonicator (Branson Ultrasonic Corporation, Danbury, Connecticut, USA) was used to sonicate the chitosan powder for 30 minutes at room temperature at 230 V. The combination also contained 150 mg/ml of distilled water. A vortex agitator was used to stir the suspension before it was administered.

2.2.5. ZnO NP preparation with a suspension of chitosan

Powdered chitosan and zinc oxide nanoparticles (10 mg/kg and 150 mg/ml) were combined and dissolved in distilled water. After that, the suspension was sonicated using an ultrasonic cleaner sonicator (Branson Ultrasonic Corporation, Danbury, Connecticut, USA) for 40 minutes at 230 V while it was at room temperature. A vortex agitator was used to stir the suspension before it was administered.

2.2.2. Experimental design

Seventy-five Adult male Wister albino Rats, weighing (180 – 200) gm, will be use in this study. The animals will be kept in temperature-controlled environments in cages made of stainless steel (25±2 ◦C temp) and we will provide free access to pelleted food and purified drinking water. After 1 week of acclimation, the rats randomly dividing into 5 groups (15 rats at each group) as following:

1- Control group (Negative control).
2- Diabetic group (Positive control) (received 45mg/kg STZ Intraperitoneal injection).
3- Diabetic and Zinc oxide nanoparticles group (received10 mg/kg ZnoNPs).
4- Diabetic and chitosan group (received 150mg/kg Chitosan).
5- Diabetic, chitosan, and Zinc oxide nanoparticles group (Chitosan + ZnoNps Capsule) (received 150 mg/kg Chitosan + 10 mg/kg ZnoNPs).

After 6 weeks, the test animals were fasted for eight hours and then given diethyl ether to put them to sleep. Blood samples were extracted from the orbital venous plexus, placed in non-heparinized tubes, centrifuged for 15 minutes at 2500 rpm, and blood sera were gathered, aliquoted, and stored at -80 °C until needed (Kumar *et al.,* 2017).

2.2.4. Histopathological Examination

After the blood was collected, the pancreas and liver were quickly removed and fixed in 10% buffered formaldehyde. After being fixed, the samples were dried, embedded in wax, and then cut into 5 micron pieces. For histological investigation, slices were stained with hematoxylin and eosin (Feldman and Wolfe, 2014). Lastly, a light microscope (Olympus BX 51, Olympus America, Melville, NY) was used to conduct the experiment at different magnifications.

2.2.5. Blood biochemical parameters:

2.2.5.1. Glucose test

2.2.5.1.1. Assessment of glucose

It is recommended that all Standards and Samples undergo duplicate analyses. It is strongly recommended to conduct a trial experiment before measuring any samples.

1) After securing the necessary number of coated wells in the holder, insert 100 µL of Standards or Samples into the appropriate well. Transfer 100 µ L of PBS (pH 7.0–7.2) into the empty control well.
2) Use just 1 µL of the Balance Solution, and mix 10 µL samples well. When the sample is bodily fluid or tissue homogenate, cell culture supernatant, this step is required.
3) 50 µL of conjugate should be added to each well; DO NOT add a blank control well. Mix well. It is important to fully mix during this stage. Cover the dish and let it sit at 37°C for an hour.

2.2.5.1.2. Assessment of Insulin

First, the plate must be opened, 100 µl of standard or sample must be added to each well, the well must be covered with a closure plate membrane, and the plate must be left to incubate for 2.5 hours at room temperature. 100 µl of the biotinylated detection antibody working solution was added to each well of the plate after four washings and the removal of the contents. The dish was given a slight shake and then allowed to stand for sixty minutes at room temperature. After that, the dish was cleaned four times, and its contents were thrown away. Following the addition of 100 µl of HRP conjugate working solution to each well, the plate was gently shaken and allowed to rest at room temperature for 45 minutes. Following four cleanings, the contents of the plate were disposed of. After that, 100 µl of ELISA detection substrate (TMB) was applied to each well. After giving the plate a quick shake, it was allowed to sit at room temperature in the dark for 30 minutes. Thirty minutes after adding 50 µl of stop solution to each well, the absorbance at 450 nm was measured. The standard curve equation was used to determine the concentration.

2.2.5.1.3. Assessment of A hemoglobin A1C (HbA1C)

1. Put 100 µL of the standard or sample into each well. Incubate for ninety minutes at 37°C.
2. Remove the liquid. Add 100 µL of detection antibody that has been biotinylated. Incubate for one hour at 37°C.
3. After three aspirations, wash.
4. Add the HRP conjugate in 100 microliters. Incubate for 30 minutes at 37°C.

2.2.5.2 Liver function test:

2.2.5.2.1 Alanine Aminotransferase (ALT)

Dimension Vista's Alanine Aminotransferase (ALT) protocol is an advancement of the IFCC's suggested ALT protocol, as noted by (Zhang *et al.,* 2015). The measurement of the change in absorbance spectrum that is directly associated with ALT levels is done using a bichromatic (340, 700 nm) rate approach (Tietz *et al.,* 2006).

2.2.5.2.2. Aspartate aminotransferase (AST)

A bichromatic (340-700 nm) rate method, a version of the protocol developed by the International Federation of Clinical Chemistry (IFCC) (Wang *et al.,* 2019), was used to assess the aspartate aminotransferase method. The absorbance spectrum change is measured using a bichromatic (340, 700 nm) rate technique, and it is directly correlated with ALT levels (Tietz *et al.,* 2006).

2.2.5.2.3. Alkaline phosphatase (ALP)

The primary reference method for assessing alkaline phosphatase catalytic activity at 37°C, as established by the International Federation of Clinical Chemistry (IFCC), serves as the foundation for the ALP technique. The alkaline phosphatase method is based on a technique that was created in 1966 by Bowers and McComb and assessed by Raj in 1977. The change in absorbance at 405 nm caused by the production of p-NP is directly connected to ALP activity and is measured using a bichromatic (405, 700 nm) rate approach because additional reactions are present in non-rate-limiting levels. Rate method (405, 700 nm) (Bowers and McComb, 1966; Raj, 1977).

2.2.5.2.4. Gamma Glutamyltransferase (GGT)

The GGT approach uses the Dimension view @ system to analyze the quantitative dimension of glutamyltransferase in human serum and plasma in vitro. The International Federation of Clinical Chemistry (IFCC) established a methodology that is adapted for glutamyltransferase (Shaw *et al.,* 1983). This change is determined by a bichromatic (405,600 nm) rate approach and is related to the activity of glutamyltransferase.

2.2.5.2.5. Lactate Dehydrogenase (LDH)

1. Prepare the reagents, samples, and standards.
2. After adding the standard and the ready samples, incubate at 37 °C for 90 minutes.
3. After two washes, add the biotinylated antibody solution and let it sit at 37 °C for an hour.
4. After three washings, add the enzyme working solution and let the mixture sit at 37 °C for thirty minutes.
5. Add the color reagent solution and incubate at 37 °C for a maximum of thirty minutes after washing five times.

Add Color Reagent C in step six.

7. After adding Color Reagent C, measure the OD with a microplate reader within ten minutes.
8. Ascertain what is contained in the test samples (Joseph *et al.,* 2001).

2.2.5.2.6. Total Bilirubin (TBIL)

The TBIL method is an adaptation of the reference method Doumas in 1987, which itself is an adaptation of the 1938 diazo method Jendrassik and Grof described. Using a bichromatic (540, 700 nm) endpoint approach, the total bilirubin absorbs at 540 nm and is quantified.

2.2.5.2.7. Total Proteins (TP)

The total protein technique is an adaptation of the biuret reaction developed by Kingsley, which Henry (2001) further refined and Henry defined as a serum treatment method. A bichromatic spectrophotometer can be used to determine the sample's total protein concentration. the end point technique at (540, 700 nm).

2.2.5.2.8 Albumin (ALB)

The dye-binding methods for bromocresol purple (BCP) outlined by (Carter, 1970; Louderback and Shanbrom, 1960) provide the basis of the albumin method. The compound absorbing at 600 nm is found using a polychromatic (600, 540, 70 nm) endpoint approach.

2.2.5.3. Oxidative stress markers:

2.2.5.3.1. Malondialdehyde (MDA) assay kit

Lipid peroxidation monitoring and reporting was made possible by the very successful technique of thiobarbituric acid reactive substances (TBARS) monitoring and prevention (Yagi, 1998). Many researchers have created the TBARS assay to evaluate a variety of methods, such as foods, medicines, and bodily fluids from humans and animals (Dawn-Linsley *et al.,* 2005).

1. Write the specimen identification number on the vial lids.
2. Transfer 100 µl of the sample halfway into a 5 ml container.
3. Swirl 100 µl of the SDS Solution into the vial to blend it.
4. Fill the bottom of each vial with 4 mL of Color Solvent.
5. To maintain the tubes upright during the boiling process, cap them and set them on a foam cushion or other similar holder. After an hour, take the vials and submerge them in the cold bath to stop the reaction. On ice, incubate for ten minutes.
6. Boil a pot of water and submerge vials for one hour.
7. To complete the reaction, take the vials out and put them in a cold bath after an hour.
8. Let it sit on ice for ten minutes to incubate. 150 µl from each vial should be placed onto the transparent or black plate.
9. Calculate the fluorescence at 550 nm and the absorbance between 530 and 540 nm.

2.2.5.3.2. Glutathione (GSH) assay kit

1. Remove the necessary strips from the zip-lock bag and let them come to room temperature. Repackage the unused strips and desiccant into the sealed aluminum foil bag and store it between 2 and 8 degrees Celsius.
2. Reserve the empty wells.
3. Fill appropriate wells (100µl per well) with samples or varying concentrations of Rat GSH standard samples; 0µg/ml wells should be filled with standard diluent. Adhesive tapes are used to seal the reaction wells, and they are then incubated for 90 minutes at 37°C.
5. Repeatedly wash the Elisa plate
6. Fill each well with 100µl of the biotinylated Rat GSH antibody liquid. Reaction wells are sealed using adhesive tapes, and they are incubated for 60 minutes at 37°C.
7. 30 minutes in advance, prepare the enzyme-conjugate liquid.
8. Three times, wash the Elisa plate
9. Pour 100µl of the enzyme-conjugate liquid into each well, excluding the blank wells. Using adhesive tape, seal the reaction wells, and then hatch them in an incubator for 30 minutes at 37°C.
10. Five times, wash the Elisa plate. 4. 30 minutes in advance, prepare the liquid biotinylated Rat GSH antibody.
11. Fill each well with 100µl of Color Reagent liquid (as well as the blank well), and hatch the eggs at 37°C in a dark incubator. Hatching can be halted when the color for a high concentration of the standard curve becomes darker and a color gradient forms. Within thirty minutes, the chromogenic process needs to be under control.
12. Fill each individual well (as well as the blank well) with 100µl of Color Reagent C. Blend thoroughly. Within ten minutes, read the OD at 450 nm.

2.2.5.3.3. Superoxide dismutase (SOD) assay kit

1. Pour 200 l of diluted Radical Detector and 10 µl of Standard (tubes A–G) into the designated wells on the plate.
2. Mix 10 µl of the well sample with 200 l of diluted Radical Detector.
3. Fill each well with diluted Xanthine Oxidase to start the reaction.
4. Shake the 96-well plate gently for a few seconds to mix. Put the plate cover back in place.
5. Use a shaker to incubate the plate for 30 minutes at room temperature. Measure the absorbance at 440–460 nm using a plate reader.

2.2.5.3.4. Catalase (CAT) assay kit

1.Formaldehyde Standard Wells: Transfer 100 µl of diluted Assay Buffer, 30 µl of methanol, and 20 µl of standard (tubes A–G) into the designated wells on the plate.
2. Positive Control Wells (bovine liver CAT): Transfer 20 l of diluted Catalase (Control), 30 l of methanol, and 100 µl of diluted Assay Buffer into each of the two wells.
3. Specimen Wells: Add 20 µl of sample, 30 µl of methanol, and 100 µl of diluted Assay Buffer to each of the two wells. To get reproducible findings, the well should have an activity of between 2-35 nmol/min/ml after adding a certain amount of CAT.
4. Fill each well with 20 µl of diluted hydrogen peroxide to start the reactions.
5. Use a shaker to incubate the plate at room temperature for 20 minutes after covering it with the plate cover.
6. Fill each well with 30 liters of potassium hydroxide and 30 liters of Catalase Purpald (Chromogen) (Item No. 707017) to halt the process.
7. After placing the plate cover on top, let it sit at room temperature for ten minutes on the shaker.
8. Transfer 10 l of Catalase Potassium Periodate (Item No. 707018) into each well. Place a plate cover over it and shake the mixture for five minutes at room temperature.
9. Determine the absorbance at 540 nm using a plate reader.

3. Statistical Analysis

IBM SPSS Statistics for Windows, version 23 was used to analyze the data, which were displayed as mean +/- standard deviation (SD) (IBM SPSS, IBM Corp., Armonk, N.Y., USA). The Shapiro-Wilk test was employed to assess the normal distribution of the data. One-Way analysis of

variance (ANOVA) was used to compare statistical data between groups, and Tukey's test was then used to compare data between groups. P-values less than 0.05 were deemed to indicate statistical significance in the results.

3. Results

3.1. Nano characterizations:

3.1.1. Scanning electron microscope and energy-dispersive spectroscopy

The powdered ZnO was morphologically investigated using scanning electron microscopy (SEM). According to Figure (1-a), the average size of ZnO particles is estimated to be 14-21 nm. The homogeneity and aggregation of the powder are depicted in the SEM image. The ZnO NPs SEM picture showed the irregularly distributed mixed-shaped particles. It has been noted that the formation of multiple small particles with varying sizes and shapes led to the formation of giant particles. The surface morphology of chitosan is depicted in Figure (1-b), where it exhibits a smooth, uniform surface with occasional fissures.

In addition to the bigger aggregates, (1-c) makes visible a vast number of individual particles varying widely in size and form.

The ZnO nanoparticles' EDX spectrum is shown in Figure (2-a). Four peaks in the EDX spectrum can be recognized as oxygen and zinc. Thus, it may be concluded that ZnO nanoparticles that are pure.

The spectrum demonstrates the existence of the three essential components-carbon, nitrogen, and oxygen—that make up the biopolymer chitosan's chemical structure (Sumaila *et al.,* 2020) Figure (2-b).

ZnO-Chitosan nanoparticles were discovered to be 100% pure and composed of zinc as well as oxygen, carbon, and nitrogen elements Figure (2-c).

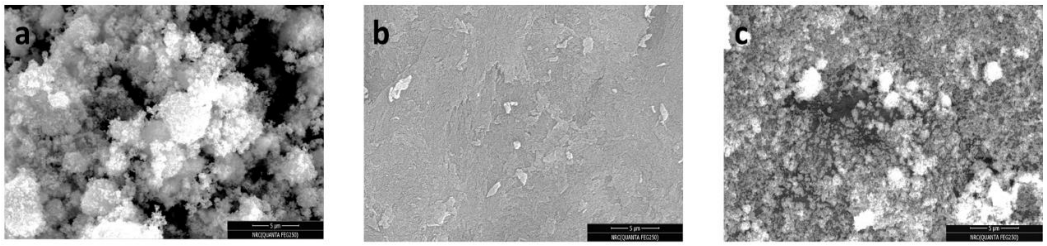

Fig.1: Scanning electron micrographs of (a) ZnO Nps (b) Chitosan (C) Chitosan & ZnO Nps.

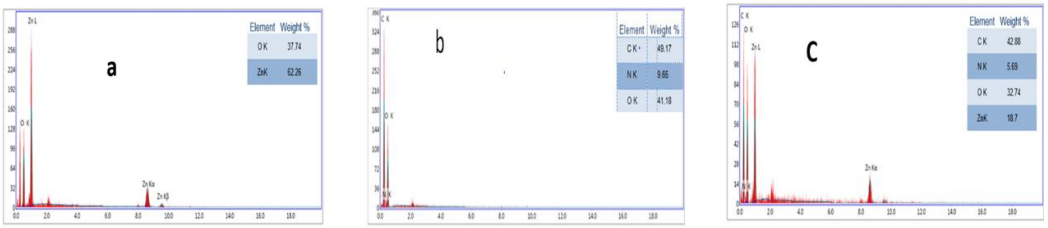

Fig.2: EDS for (a) ZnO Nps (b) Chitosan (C) Chitosan & ZnO Nps.

4.1.2. TEM analysis

ZnO nanoparticles, chitosan, and ZnO-Chitosan nanoparticles were measured to be 17.5, 3.75, and 17.8 nm, respectively, Figure (3). These results are consistent with the XRD data.

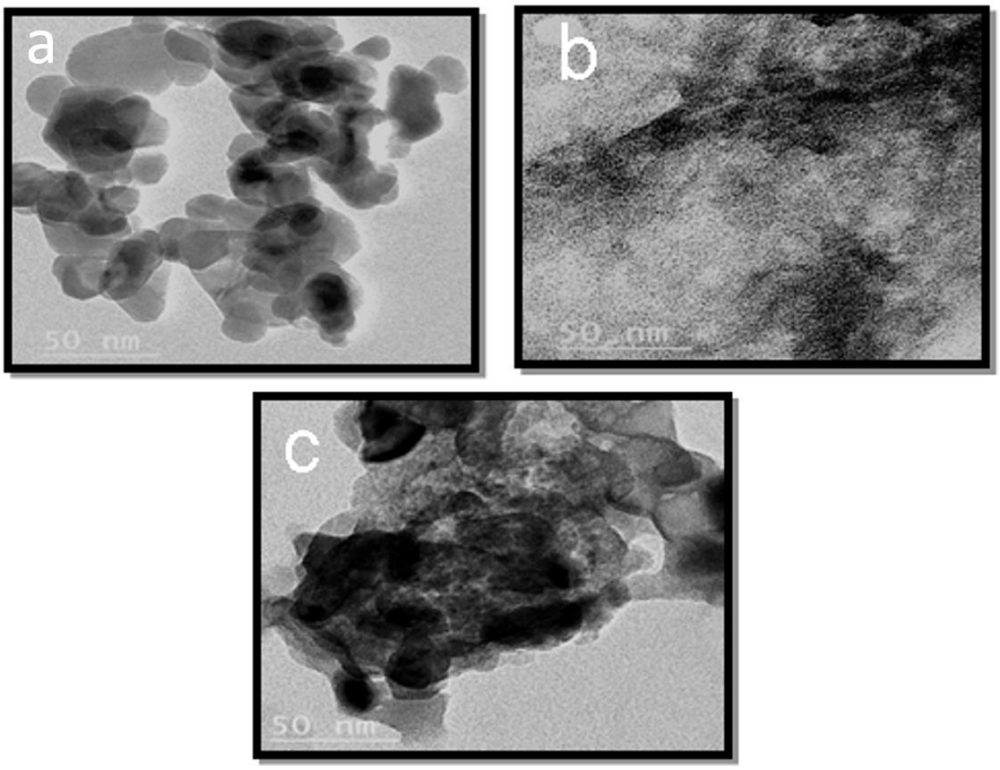

Fig. 3: Transmission electron micrographs of (a) ZnO Nps (b) Chitosan (C) Chitosan & ZnO Nps.

3.1.3. XRD

3.1.3.1. ZnO NPs

The ZnO nanoparticles' hexagonal Zincite structure was confirmed by the measurement of their XRD pattern, as depicted in figure (4) and in accordance with the standard JCPDS file of the ZnO zincite phase (JCPDs No. 36 - 451). The 2 Theta values of 31.77°, 34.42°, 36.26°, 47.54°, 56.61°, 62.88°, 66.36°, 67.96°, 69.1°, 72.56°, and 76.98° corresponded to the lattice planes (100), (002), (101), (012), (110), (013), (200), (112), (004), and (202). These values were seen as the diffraction peaks (Chaudhari *et al.,* 2022; Walunj *et al.,* 2023; Endah *et al.,* 2023). Using the Debye-Scherrer formula, the crystallite size of the nanoparticles for the (101) peak was determined to be 17.5 nm Figure (4-a).

3.1.3.2. Chitosan

X-ray Diffraction (XRD) analysis Standard chitosan from Sigma Aldrich has peaks in the XRD pattern at 2θ of 20° as Figure 1 shows two distinctive diffraction peak at 2θ = 20° that linked to the (212) plane (Pokhrel *et al.,* 2016). Chitosan was effectively synthesized and appears to be partly crystalline polysaccharide, according to the XRD pattern (Günister *et al.,* 2007). The crystallite size (D) of chitosan (CS) has been calculated by using the Debye – Scherrer formula. The crystallite size of chitosan (CS) is 3.75 nm Figure (4-b).

4.1.3.3. Zno + Chitosan

The X-ray diffraction (XRD) pattern of ZnO and ZnO-Chitosan nanoparticles revealed multiple Bragg's reflections peaks attributed to ZnO and chitosan, as shown in Peaks appeared at 2θ values of 31.8°, 34.5°, 36.3°, 47.7°, 56.8°, 63.1° and 67.7°, 68.2°, 72.9°, 77.2°, respectively, of hexagonal structure of ZnO nanoparticles, matching to standard spectrum of ZnO (JCPDs No. 36 -1451) In the ZnO-Chitosan composite, the peak of Bragg's reflections owing to chitosan was seen at a 2θ value of 20° (Javed *et al.,* 2020). Using the Debye-Scherrer formula, the average crystallite sizes of ZnO-Chitosan nanoparticles were found to be 17.9 nm Figure (4-c).

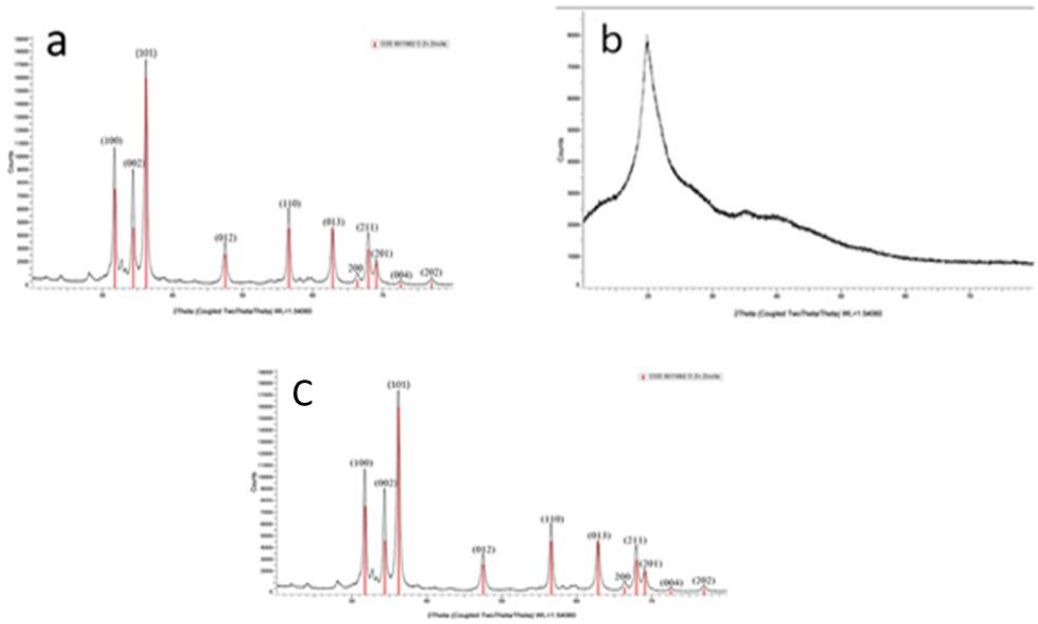

Fig. 4: XRD (a) ZnO Nps (b) Chitosan (C) Chitosan & ZnO

3.3. Histopathological examination of Pancreas

A histological investigation and a blood biochemical analysis were conducted to validate the effectiveness of fenugreek seed extract combined with ZnO nanoparticles in the management of diabetes mellitus in rats. The histologically controlled pancreatic structure is characterized by narrow spacing between lobules. The exocrine sections included embedded Langerhans islets (Figure 5-G1). The pancreas of the diabetic rat exhibited a notable decrease in islets of Langerhans (IL) together with notable degenerative alterations and necrotic tissue in all the islets. Additionally, the acini displayed a notable atrophy along with degenerative, enlarged spaces between lobules, and vaculation alterations (Figure 5- G2). The pancreas of rats given zinc oxide nanoparticle treatment displayed a return to normal size of the islets of Langerhans (IL), along with notable peripheral hyperplasia, minor central vaculation, and necrotic alterations that clearly displayed the distribution and appearance of beta cells (Figure 5- G3). In the group that received chitosan treatment, the pancreas displayed a return to normal in terms of the size of the islets of Langerhans (IL), the distribution of endocrine cells, the presence of moderate necrotic tissue, and the appearance and distribution of beta cells in the central vaculation (Figure 5- G4). The pancreas of the ZnO NP-treated rat displayed a normal histologic appearance, with normal size, population, and architecture. There was some minor islet capillary congestion, a few cells that were either hypertrophied or apoptotic, and closely spaced lobules (Figure 5- G5).

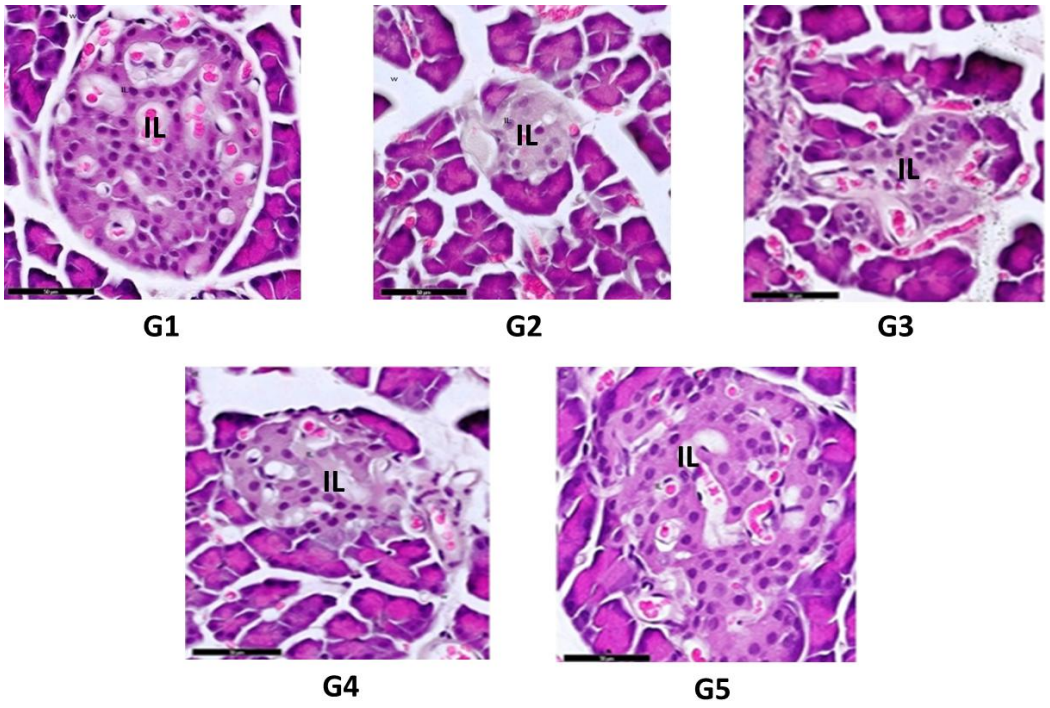

Fig. 5: Photomicrograph of pancreatic tissues staining H&E (scale bar 50 µm, 400 magnification). (G1) Control group, (G2) Diabetic group (received STZ), (G3) Diabetic + ZnO NPs, (G4) Diabetic + Chitosan, (G5) Diabetic + ZnO NPs + Chitosan. IL: Islet Langerhans.

3.4. Histopathological examination of Liver

Rat diabetes mellitus was successfully treated using chitosan encapsulation with ZnO NPs, according to blood biochemical analysis and histopathological study.

The histological illustration (Figure 6) shows that the livers of normal rats have regular histoarchitecture. The hepatic parenchyma and blood sinusoids appeared normal with a typical distribution of Kupffer cells, in contrast to the livers of diabetic rats, which displayed prominent necrotic changes, dilatation of liver sinusoids, activation of Kupffer cells, and cytoplasmic vacuolization of hepatocytes along with congested central veins, hemorrhagic changes, infiltration of inflammatory cells, some apoptotic changes, and nuclear karyolitic changes. Improvements to differing degrees were noted after treatment. In addition to a modest number of Kupffer cells and moderate degenerative changes, the liver of the ZnO NPs-treated group showed moderate hepatic sinusoids dilatation. In the group treated with chitosan, the liver's histoarchitecture was largely normal, exhibiting minimal deterioration and necrobiotic changes. Moreover, there was a slight increase in the number and distribution of blood sinusoids in addition to a slight dilatation of them. The chitosan-treated ZnO NPs liver group showed normal tissue histoarchitecture, with slightly enlarged blood sinusoids (BS), normal distribution and number of Kupffer cells, and moderately clogged central veins (CV).

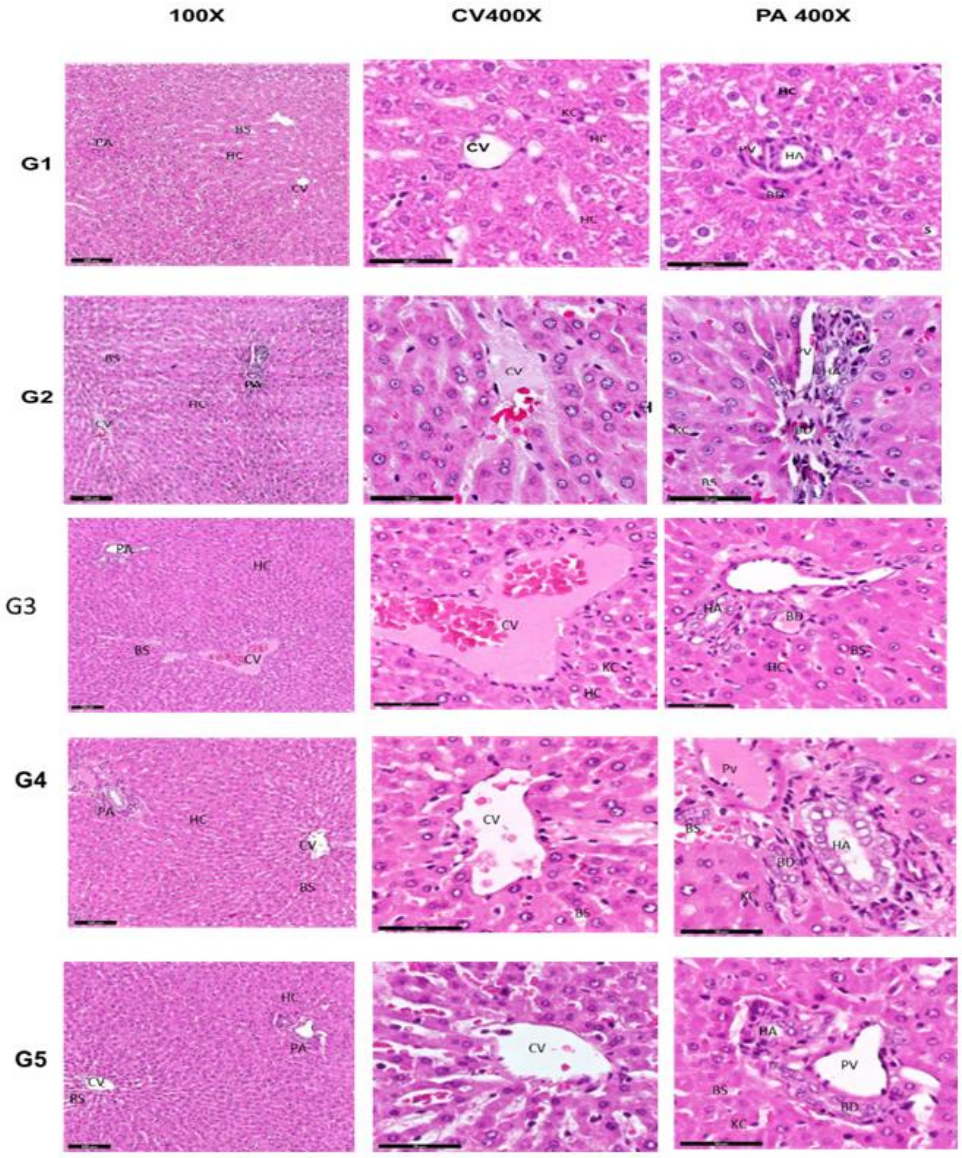

Fig. 6: Hepatocyte slices stained with H&E (magnification 400 x, scale bar 50 µm,). In Group I: Normative references, (G2) Group 2: STZ treated diabetic control, (G3) Group 3: ZnO NPs+ Diabetic, (G4) group 4: Chitosan + Diabetes, (G5) Group 5: ZnO NPs produced from Diabetic + Chitosan. Where HA stands for hepatic artery, BD for dile duct,HC for hepatic for kupffer cell, and PA for portal area.

3.5. Blood Biochemical Parameters

3.5.1. blood glucose

Table (1) showed the effects of ZnO and Chitosan administration on blood glucose, insulin and HBA1C levels in different studied groups. The blood glucose levels were significantly increased in STZ, STZ + ZnO, STZ + Chitosan groups but was significantly decreased in STZ + ZnO + Chitosan group versus control (p <0.001). Blood glucose levels were significantly increased in STZ group versus STZ + ZnO, STZ + Chitosan and STZ + ZnO + Chitosan groups (p <0.001).

Table 1: Effects of ZnO and Chitson adminstration on glycemic control in diabetic male rats in different studied groups.

Parameters	Control	STZ	STZ+ ZnO	STZ + Chitosan	STZ + ZnO + Chitosan
Glucose (mg/dl)	100.17±0.14	330.18±0.14 ^{a***}	119.08±0.07 ^{a***,b***}	115.22±0.17 ^{a***,b***,c***}	69.15±0.11 ^{a***,b***,c***,d***}
Insulin (mIU/L)	20.42±0.02	2.85±0.04 ^{a***}	20.42±0.02 ^{b***}	15.83±0.03 ^{a***,b***,c***}	22.53±0.03 ^{a***,b***,c***,d***}
HbA1C (%)	6.09±0.07	9.45±0.04 ^{a***}	4.22±0.02 ^{a***,b***}	4.83±0.03 ^{a***,b***,c***}	4.32±0.02 ^{a***,b***,c**,d***}

Data were respresented as mean +/- standard deviation (SD). a: Significance versus control group; b: significace versus STZ; c: significance versus STZ+ ZnO; d: significance versus STZ + Chitosan. ***P* <0.010 and ****P* <0.001.

Blood glucoses levels were significantly descreased in STZ + ZnO, STZ + Chitosan versus STZ + Chitosan and STZ + ZnO (p <0.001) and in STZ + Chitosan versus STZ + ZnO groups (p <0.001) (Figure 7).

However, serum insulin were significantly decreased in STZ, STZ + ZnO and STZ + Chitosan but significant increased in STZ + ZnO + Chitosan groups versus control (p <0.001 for all).

serum insulin levels were increased in STZ + ZnO, STZ + Chitosan and STZ + ZnO + Chitosan groups versus STZ group (p <0.001 for all).

Serum insulin levels were increased in STZ + ZnO +Chitosan versus STZ + Chitosan and STZ + ZnO and in STZ + ZnO versus STZ + Chitosan groups (p <0.001) (Figure 8).

HbA1C levels were significantly decreased in STZ + ZnO, STZ + Chitosan and STZ + ZnO + Chitosan groups versus control (p <0.001). HbA1C levels were significantly increased in STZ group versus STZ + ZnO, STZ + Chitosan and STZ + ZnO + Chitosan groups (p <0.001).

HbA1C levels were significantly increased in STZ + Chitosan versus STZ + ZnO and STZ + ZnO + Chitosan groups (p <0.001) but were significantly decreased in STZ + ZnO versus STZ + ZnO + Chitosan groups (p <0.010) (Figure 9).

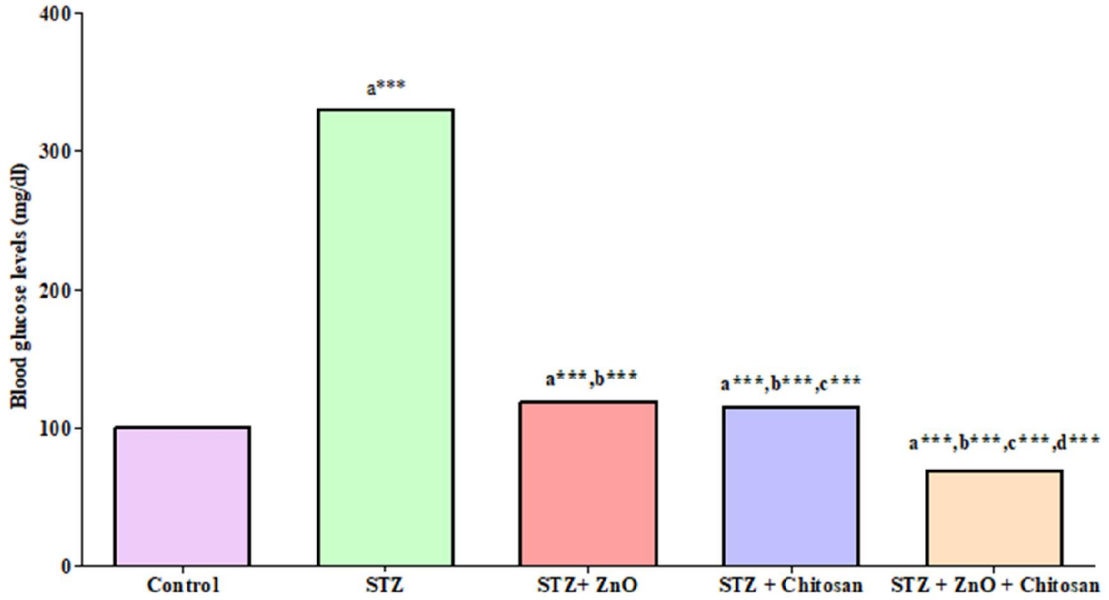

Fig: 7: Effects of ZnO and Chitson administration on blood glucose (mg/dl) levels in diabetic male rats in different studied groups.

Data were represented as mean +/- standard deviation (SD). **a:** Significance versus control group; **b:** Significance versus STZ; **C:** Significance versus STZ + ZnO; **d:** Significance versus STZ + ZnO + Chitosan. ***:*P< 0.001*.

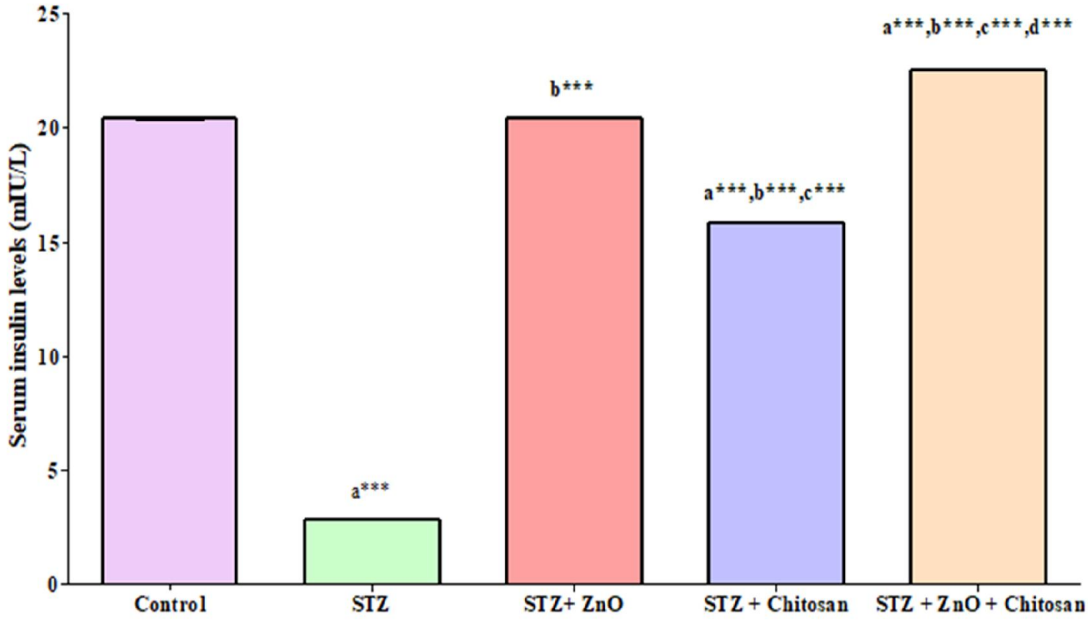

Fig: 8: Effects of ZnO and Chitson administration on serum insulin(mIU/L) levels in diabetic male in in different studied groups.

Data were represented as mean +/- standard deviation **(SD)**. **a:** Significance versus control group; **b:** Significance versus STZ; **C:** Significance versus STZ + ZnO; **d:** Significance versus STZ + ZnO + Chitosan. ***:*P< 0.001*.

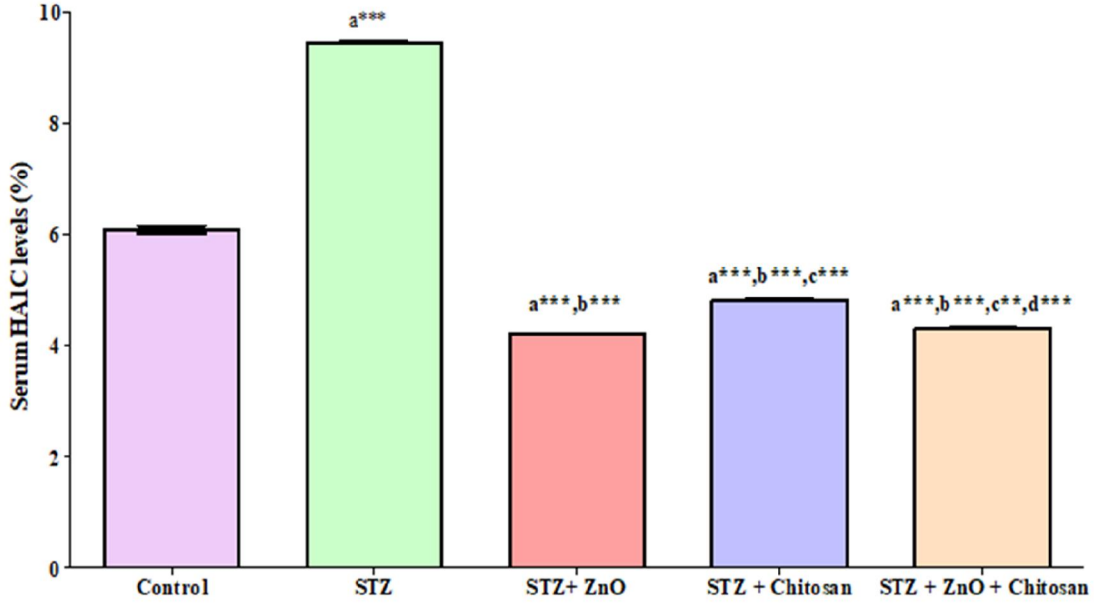

Fig. 9: Effects of ZnO and Chitson adminstration on serum levels of HA1C (%) in diabetic male rats in different studied groups.

Data were represented as mean +/- standard deviation (SD). a: Significance versus control group; b: significance versus STZ; c: significance versus STZ + ZnO d: significance versus STZ + Chitosan. *P <0.010 and **p <0.001.

4.5.2. Liver function

Table (2) showed the effects of ZnO and Chitosan administration on liver function tests as ALT, AST, ALP, GGT, LDH, total bilirubin, total proteins and albumin serum levels in different studied groups. The serum levels of ALT, AST, ALP, GGT, LDH were significantly increased STZ, STZ + ZnO, STZ + Chitosan groups versus control (p <0.001). ALT, AST, ALP, GGT, LDH levels were significantly decreased in STZ + ZnO, STZ + Chitosan and STZ + ZnO + Chitosan groups versus STZ group (p <0.001).

Table 2: Effects of ZnO and Chitson adminstration on liver function tests in diabetic male rats in different studied groups.

Parameters	Control	STZ	STZ+ ZnO	STZ + Chitosan	STZ + ZnO + Chitosan
ALT(U/L)	18.47±0.06	70.19±0.15 ^{a***}	35.23±0.03 ^{a***,b***}	32.65±0.04 ^{a***,b***,c***}	17.42±0.02 ^{a***,b***,c***,d***}
AST(U/L)	23.52±0.22	100.10±0.09^{a***}	45.23±0.04 ^{a***,b***}	41.11±0.09 ^{a***,b***,c***}	25.64±0.04 ^{a***,b***,c***,d***}
ALP(U/L)	50.09±0.07	121.19±0.15^{a***}	63.23±0.03 ^{a***,b***}	55.10±0.08 ^{a***,b***,c***}	46.56±0.05 ^{a***,b***,c***,d***}
GGT (U/L)	14.66±0.05	61.18±0.14 ^{a***}	21.10±0.08 ^{a***,b***}	16.42±0.02 ^{a***,b***,c***}	14.44±0.04 ^{a***,b***,c***,d***}
LDH (U/L)	180.19±0.15	590.18±0.15^{a***}	211.18±0.16 ^{a***,b***}	190.19±0.15 ^{b***,c***}	174.11±0.09 ^{a***,b***,c***,d***}
Total bilirubin (mg/dl)	0.54±0.00	1.89±0.00 ^{a***}	0.60±0.01 ^{a*,b***}	0.56±±0.03 ^{b***}	0.52±0.00 ^{b***,c***,d*}
Total proteins (g/dl)	6.12±0.01	5.43±0.03 ^{a***}	5.44±0.03 ^{a***}	5.63±0.03 $^{a*** ,b***,c***}$	5.83±0.03 ^{a***,b***,c***,d***}
Albumin (g/dl)	3.52±0.02	2.32±0.02 ^{a***}	2.53±0.03 ^{a***,b***}	2.82±0.02 ^{a***,b***,c***}	3.93±0.03 ^{a***,b***,c***,d***}

Data were respresented as mean +/- standard deviation (SD). a: Significance versus control group; b: significace versus STZ; c: significance versus STZ+ ZnO; d: significance versus STZ + Chitosan. **P <0.010 and ***P <0.001.

ALT, AST, ALP, GGT, LDH levels were significantly increased in STZ + ZnO and STZ + Chitosan versus STZ + ZnO +Chitosan groups (p <0.001) and in STZ + ZnO versus STZ + Chitosan (p <0.001) (Figure 10-14).

The serum levels of total bilirubin were significantly increased STZ and STZ + Chitosan groups versus control (p <0.001 and p <0.050). Total bilirubin levels were significantly decreased in STZ + ZnO, STZ + Chitosan and STZ + ZnO + Chitosan groups versus STZ group (p <0.001).

Total bilirubin levels were significantly increased in STZ + ZnO and STZ + Chitosan versus STZ + ZnO +Chitosan groups (p <0.001 and p <0.050) (Figure 15).

The serum levels of total proteins were significantly decreased STZ, STZ + ZnO, STZ + Chitosan and STZ + ZnO + Chitosan groups versus control (p <0.001). Total proteins were significantly decreased in STZ group versus STZ + Chitosan and STZ + ZnO + Chitosan groups (p <0.001).

Total protein levels were significantly increased in STZ + ZnO + Chitosan group versus STZ + ZnO and STZ + Chitosan groupd (p <0.001) and in STZ + Chitosan versus STZ + ZnO (p <0.001) (Figure 16).

Albumin serum levels were significantly decreased STZ, STZ + ZnO and STZ + Chitosan but significantly increased in STZ + ZnO + Chitosan groups versus control (p <0.001).

Albumin levels were significantly decreased in STZ group versus STZ + ZnO, STZ + Chitosan and STZ + ZnO + Chitosan groups (p <0.001).

Albumin levels were significantly increased in STZ + ZnO + Chitosan versus STZ + ZnO and STZ + Chitosan groups (p <0.001) and in STZ + Chitosan versus STZ + ZnO (p <0.001) (Figure 17).

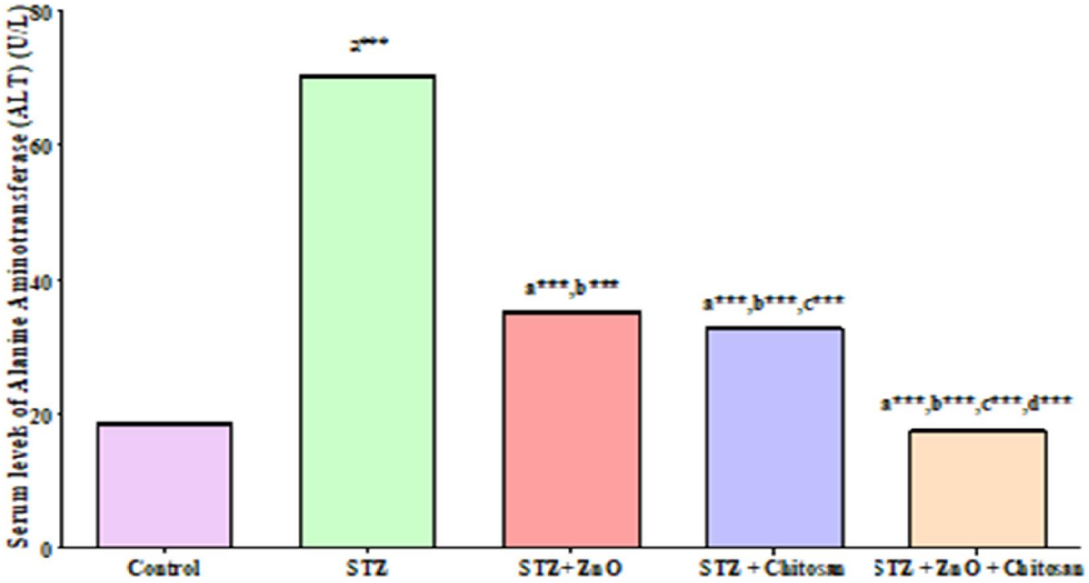

Fig. 10: Effects of ZnO and Chitson adminstration on ALT(U/L) levels in diabeticmale rats in different studied groups.

Data were respresented as mean +/- standard deviation (SD). a Significance versus control group: b: significace versus STZ; c. significance versus STZ+ ZnO; d significance versus STZ - Chitosan ***P <0.001.

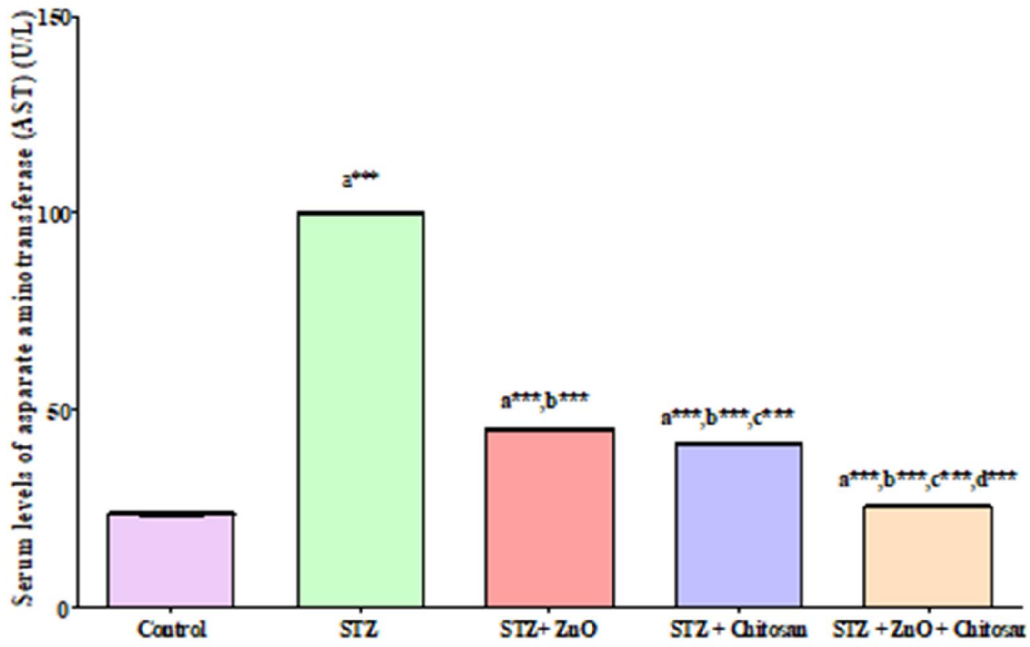

Fig. 11: Effects of ZnO and Chitson adminstration on AST (U/L) levels in diabetic male rats in different studied groups.

Data were respresented as mean +/- standard deviation (SD). a: Significance versus control group; b: significace versus STZ; c: significance versus STZ+ ZnO; d significance versus STZ+Chitosan ***P <0.001.

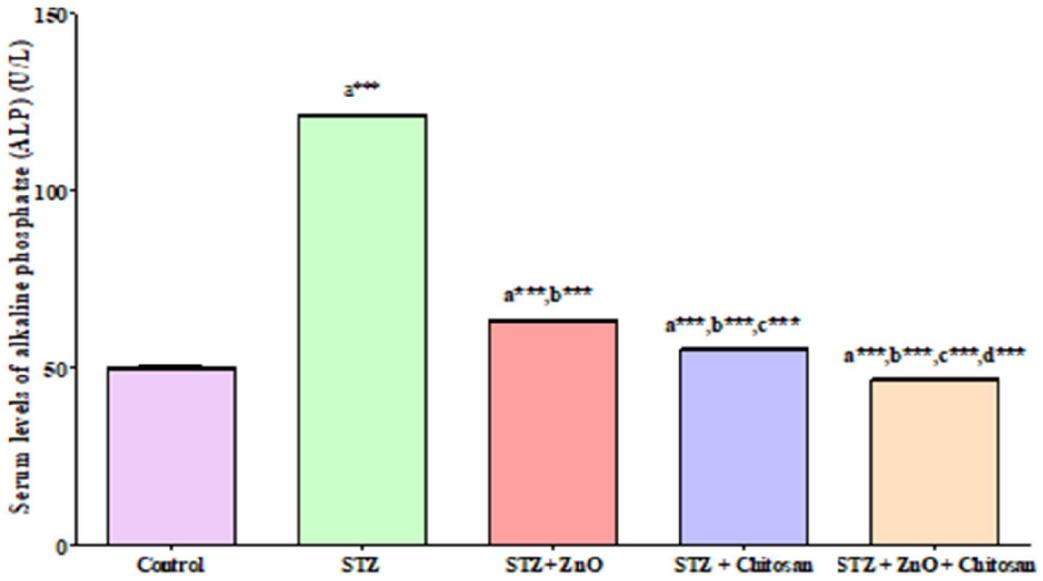

Fig. 12: Effects of ZnO and Chitson adminstration on ALP (U/L) levels in diabetic male rats in different studied groups.

Data were respresented as mean +/- standard deviation (SD). a: Significance versus control group; b: significace versus STZ; c: significance versus STZ+ ZnO; d significance versus STZ+Chitosan. ***P<0.001.

Fig. 13: Effects of ZnO and Chitson adminstration on GGT (U/L) levels in diabetic male rats in different studied groups.

Data were respresented as mean +/- standard deviation (SD). a Significance versus control group; b: significace versus STZ; c. significance versus STZ+ ZnO: d significance versus STZ-Chitosan ***P<0.001.

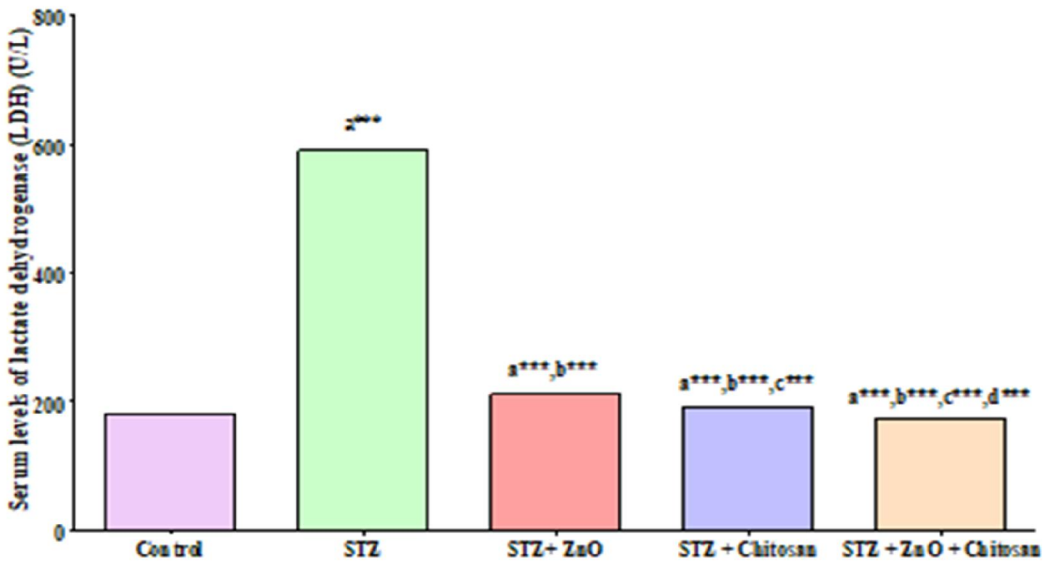

Fig. 14: Effects of ZnO and Chitson adminstration on LDH (U/L) level sin diabetic male rats in different studied groups.

Data were respresented as mean -- standard deviation (SD). a Significance versus control group; b: significace versus STZ; c significance versus STZ+ ZnO; d significance versus STZ-Chitosan ***P <0.001.

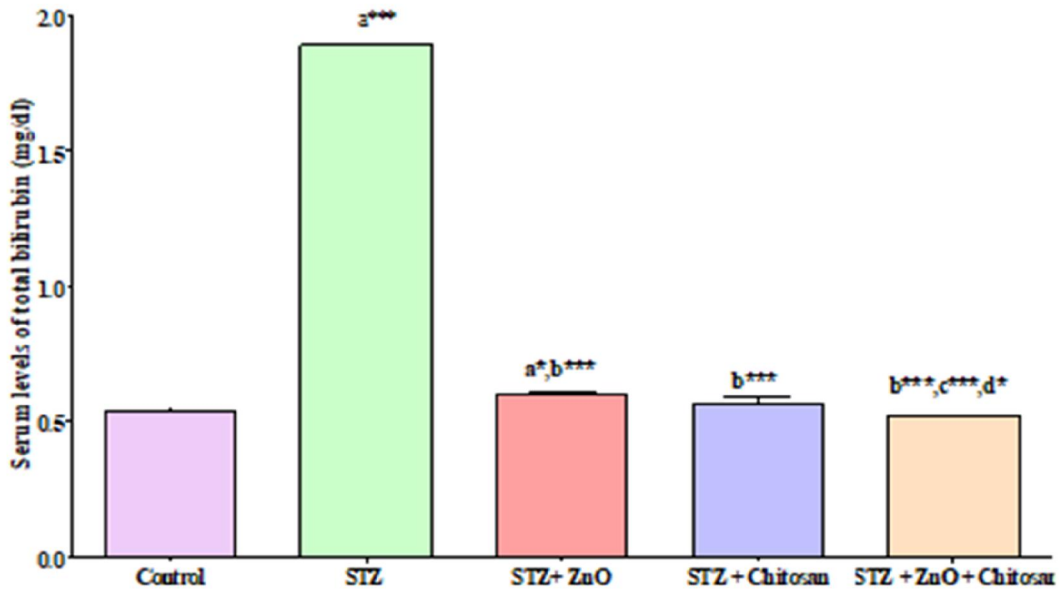

Fig. 15: Effects of ZnO and Chitson adminstration on total bilirubin (mg/dl) levels in diabetic male rats in different studied groups.

Data were respresented as mean +/- standard deviation (SD). a: Significance versus control group; b: significace versus STZ; c significance versus STZ+ ZnO; d significance versus STZ+Chitosan. * P<0.001.

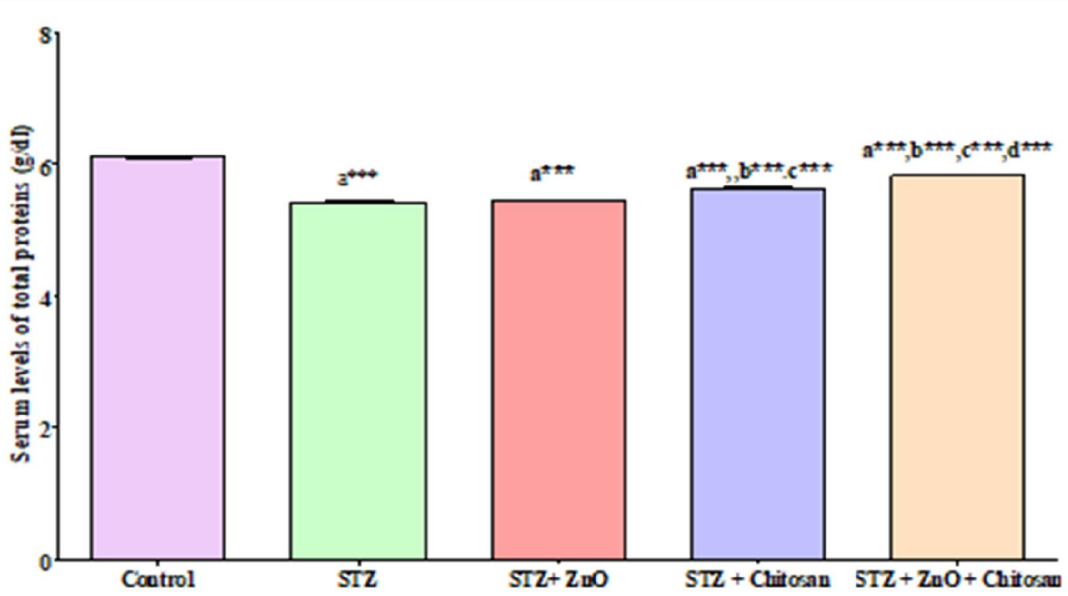

Fig. 16: Effects of ZnO and Chitson adminstration on total proteins (g/dl) levels in diabetic male rats in different studied groups.

Data were respresented as mean +/- standard deviation (SD). a: Significance versus control group; b. significace versus STZ; c significance versus STZ+ ZnO; d: significance versus STZ + Chitosan ***P <0.001.

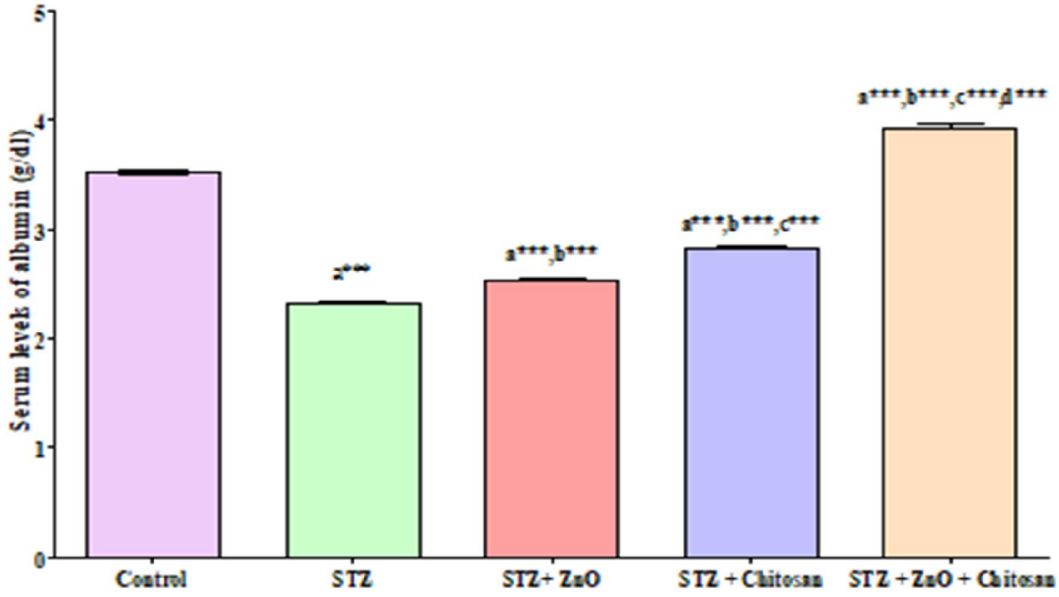

Fig. 17: Effects of ZnO and Chitson adminstration on albumin (g/dl) levels in diabetic male rats in different studied groups.

Data were respresented as mean - standard deviation (SD). a: Significance versus control group, b: significace versus STZ; c: significance versus STZ+ZnO; d: significance versus STZ+Chitosan. ***P <0.001.

3.5.3. Oxidative stress markers

Table (3) showed the effects of ZnO and Chitosan administration on MDA, GSH, SOD and CAT serum levels in different studied groups.

MDA serum levels were significantly increased STZ, STZ + ZnO and STZ + Chitosan groups but significantly decreased in STZ + ZnO + Chitosan versus control (p <0.001).

MDA levels were significantly increased STZ versus STZ + ZnO, STZ + Chitosan and STZ + ZnO + Chitosan (p <0.001).

MDA levels were significantly increased in STZ + Chitosan and STZ + ZnO versus STZ + ZnO + Chitosan and in STZ + ZnO versus STZ + ZnO + Chitosan (p <0.001) (Figure 18). GSH serum levels were significantly decreased in STZ, STZ + ZnO and STZ + Chitosan and STZ + ZnO + Chitosan groups versus control (p <0.001).

GSH levels were significantly increased in STZ + ZnO, STZ + Chitosan and STZ + ZnO + Chitosan groups versus STZ group (p <0.001), in STZ + ZnO + Chitosan versus STZ + Chitosan and STZ + ZnO groups (p <0.001) and in STZ + Chitosan versus STZ + ZnO group (p <0.001) (Figure 19).

Table 3: Effects of ZnO and Chitson adminstration on oxidative stress markers in diabetic male rats in different studied groups.

Parameters	Control	STZ	STZ+ ZnO	STZ + Chitosan	STZ + ZnO + Chitosan
MDA (nmol/ml)	0.44±0.00	1.66±0.00 ^{a***}	0.82±0.00 ^{a***,b***}	0.78±0.00 ^{a***,b***,c***}	0.41±0.00 ^{a***,b***,c***,d***}
GSH (ng/ml)	19.11±0.09	4.09±0.07 ^{a***}	9.82±0.02 ^{a***,b***}	12.35±0.04 ^{a***,b***,c***}	17.42±0.02 ^{a***,b***,c***,d***}
SOD (U/ml)	186.11±0.09	90.13±0.10 ^{a***}	132.15±0.12 ^{a***,b***}	141.13±0.10 ^{a***,b***,c***}	190.14±0.11 ^{a***,b***,c***,d***}
CAT (Mu/L)	119.13±0.10	85.10±0.08 ^{a***}	100.15±0.12 ^{a***,b***}	104.16±0.13 ^{a***,b***,c***}	123.13±0.10 ^{a***,b***,c***,d***}

Data were respresented as mean +/- standard deviation (SD). a: Significance versus control group; b: significace versus STZ; c: significance versus STZ+ ZnO; d: significance versus STZ + Chitosan. ***:P <0.001.

SOD and CAT serum levels were significantly decreased in STZ, STZ + ZnO, STZ + Chitosan groups but was significantly increased in STZ + ZnO + Chitosan groups versus control (p <0.001).

SOD and CAT levels were significantly increased in STZ + ZnO, STZ + Chitosan and STZ + ZnO + Chitosan groups versus STZ group (p <0.001), in STZ + ZnO + Chitosan group versus STZ + ZnO and STZ + Chitosan groups (p <0.001) and in STZ + Chitosan versus STZ + ZnO group) (p <0.001) (Figure 20- 21).

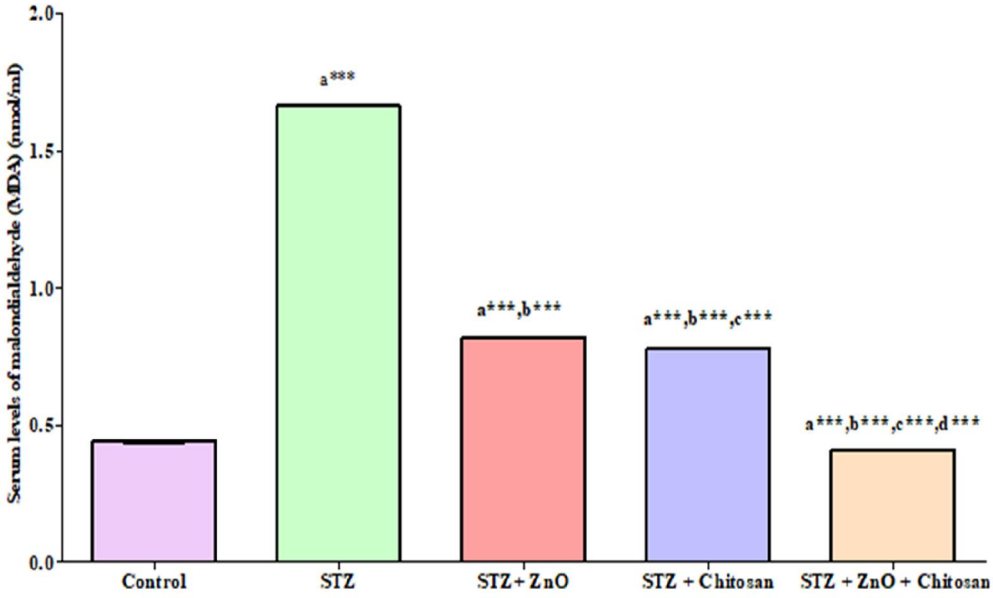

Fig. 18: Effects of ZnO and Chitson adminstration on MDA (nmol/ml) levels in diabetic male rats in different studied groups.

Data were respresented as mean +/- standard deviation (SD). a: Significance versus control group; b: significace versus STZ: c: significance versus STZ+ZnO: d: significance versus STZ + Chitosan. *:P<0.001.

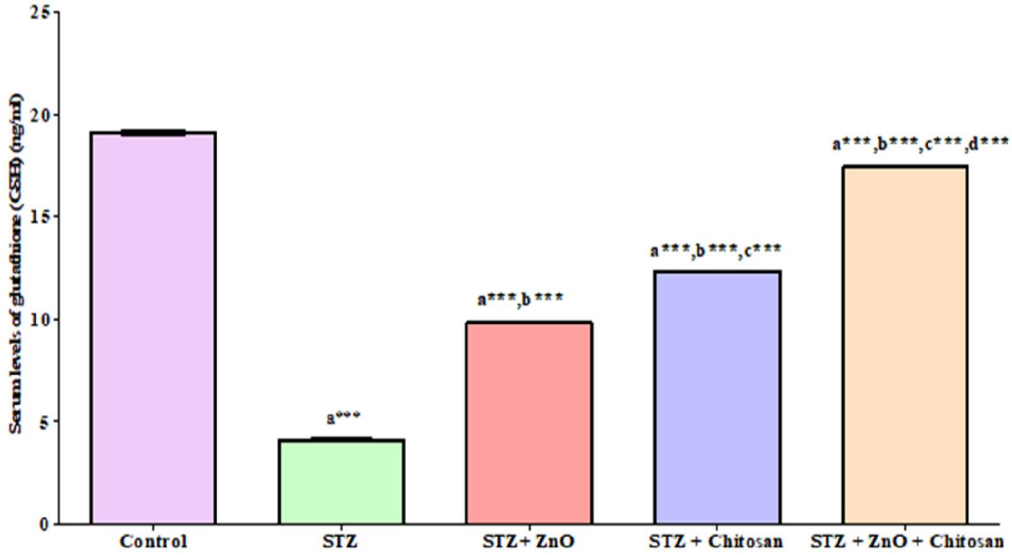

Fig. 19: Effects of ZnO and Chitson adminstration on GSH (ng/ml) levels in diabetic male rats in different studied groups.

Data were respresented as mean +/- standard deviation (SD). a: Significance versus control group; b: significace versus STZ; c: significance versus STZ+ZnO; d: significance versus STZ + Chitosan. *:P<0.001.

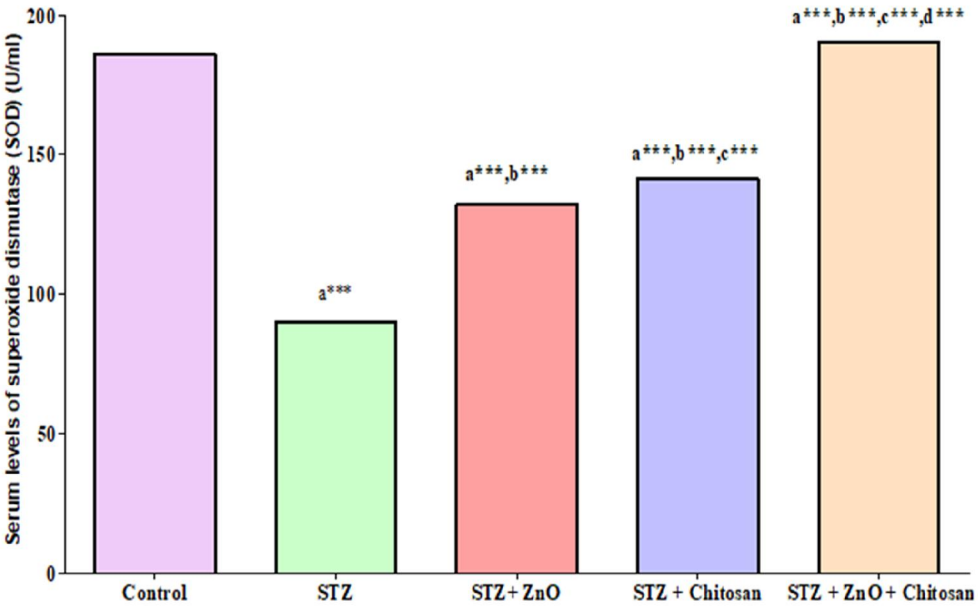

Fig. 20: Effects of ZnO and Chitson adminstration on SOD (U/ml) levels in diabetic male rats in different studied groups.

Data were respresented as mean +/- standard deviation (SD). a: Significance versus control group: b: significace versus STZ: c: significance versus STZ+ ZnO: d: significance versus STZ + Chitosan. *:P<0.001.

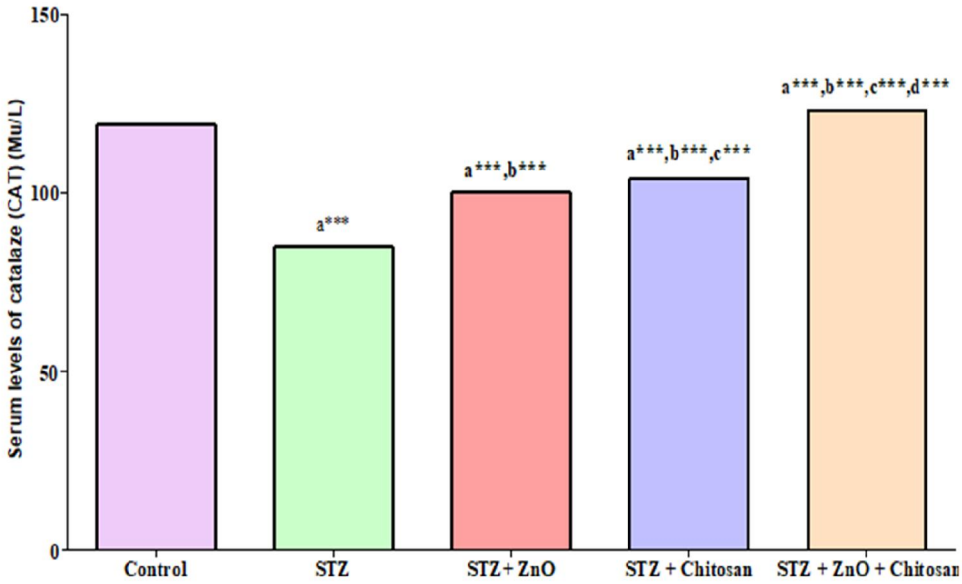

Fig. 21: Effects of ZnO and Chitson adminstration on CAT (Mu/L) levels in diabetic male rats in different studied groups.

Data were respresented as mean +/- standard deviation (SD). a: Significance versus control group; b: significace versus STZ: c: significance versus STZ+ ZnO; d: significance versus STZ + Chitosan. *:P<0.001.

4. Discussion

ZnO-NP crystallinity, as well as their structural surface morphology, size, size distribution, form, and dispersion, can all be effectively determined using a scanning electron microscope, which is widely utilized for high-resolution nanomaterials (Liou *et al.,* 2022). SEM pictures are extremely

useful for topological assessment of ZnO nanoparticles, depending on the high magnification, big field depth, and electron density of the surface (Mona *et al.,* 2018). The powdered ZnO nanoparticles were morphologically examined using scanning electron microscopy (SEM). ZnO nanoparticles are estimated to have an average size of roughly 18.5 nm, as seen in Figure (1) The homogeneity and aggregation of the powder are depicted in the SEM image. ZnO nanoparticles were found to have a similar structure by (Kim *et al.,* 2009; Ong *et al.,* 2018; Yedurkar *et al.,* 2016).

Due to the various peaks on the X-ray spectra resulting from the unique structural features of each element, EDS analysis is becoming increasingly important (Taziwa *et al*. 2017; Lai *et al*., 2021; Heidari *et al*., 2023). This EDS approach can be used to determine the purity of ZnO nanoparticles (Bala *et al.,* 2015).

The ZnO nanoparticles' EDS spectra is shown in Figure (2-a). Four peaks in the EDS spectrum can be recognized as oxygen and zinc. Thus, it may be concluded that pure ZnO nanoparticles, which concur with the information gathered by certain studies (Nozipho *et al.,* 2023; Albarakaty *et al.,* 2023)

Figure (2-c) showed that while the ZnO NPs with chitosan peaks are identified as carbon, hydrogen, oxygen, and zinc, the EDS spectrum of chitosan exhibits three peaks that must be identified as carbon, oxygen, and nitrogen. Our findings are consistent with evidence from earlier research (Nandanwar *et al.,* 2022; Phuong *et al.,* 2023)

The interaction between the highly developed high density electron bean and nanomaterial is the foundation for TEM characterization (Malatesta., 2021). The electron beam and sample interact to create a picture that can be used to assess the shape and size of nanoparticles (Aljabali *et al.,* 2018). Using TEM, Demissie *et al.* (2020) reported seeing spherically formed agglomerated ZnO NPs. The size of ZnO nanoparticles, chitosan, and ZnO-Chitosan nanoparticles were determined to be 17.5, 3.75, and 17.8 nm, respectively. These findings from the XRD investigation were validated by TEM. The literature (Vijayakumar *et al.,* 2016; Vijayakumar *et al.,* 2018; Vijayakumar *et al.,* 2020; Zewde and Geremew, 2022; Zhou *et al.,* 2023) contains spherical and hexagonal-shaped ZnO NPs.

The conclusions gained from electron microscopy analyses agreed with the outcomes of the XRD studies. The results of XRD are thought to be supported by the data from electron microscopy investigations.

Histological slices of the pancreas from diabetic rats administered ZnO NPs demonstrate the presence of the islands of Langerhans, which are more defined and exhibit little cell necrosis. The fact that pancreatic tissues in rats given ZnO NPs showed improvement suggests that zinc oxide is useful in preventing damage to pancreatic tissues, which enhances insulin output and lessens the metabolic harm brought on by diabetes (Maret, 2017).

Our findings are consistent with (Afify *et al.,* 2019), which found that a considerable drop in serum insulin levels is linked to a significant rise in blood glucose levels in the diabetic group after STZ injection.

El-Gharbawy *et al.* (2016) found that the fact that diabetic rats had insulin deficit could potentially account for the elevated blood glucose level that followed STZ injection.

Additionally, the results we got are consistent with Afify *et al.'s* (2019) study that the diabetic group had a considerably higher level of glycated hemoglobin (HbA1-C) than the control group.

The current study's findings demonstrated that STZ-diabetic rats had a considerably higher level of HbA1c than treatment groups, which was at odds with prior findings along the same line (El-Gharbawy *et al.,* 2016). This demonstrated how ZnONPs had a hypoglycemic effect by lowering blood glucose and, thus, lowering the quantity of glycosylated hemoglobin.

According to Aziz *et al.* (2013), there was a considerable drop in serum insulin levels after STZ injection, which was accompanied by a large increase in blood glucose levels in the diabetic group shown that the autoimmune-mediated loss of pancreatic beta-cells results in insulin insufficiency, which is a cause of diabetes.

As evidenced by the improvement in the histological alterations of the pancreas, liver, and kidneys as well as the restoration of BG and serum insulin levels following treatment, ZnO-NPs successfully corrected diabetes-induced pancreatic injury. The results indicate that ZnO-NPs may be able to lower the health risks related to diabetes (Shaban *et al.,* 2022).

It's interesting to note that ZnONPs can function as insulin secretagogues because they don't carry the risk of hypoglycemia in living things (Umrani and Paknikar 2014). There are various possible pathways for ZnO NPs, one of which could be enhanced glucose tolerance. First,

administering ZnO NPs may block the intestinal α-glucosidase enzyme, which would reduce the absorption of glucose. Second, there may be a decrease in blood glucose levels due to an increase in the liver's uptake of glucose and its subsequent storage (glycogenesis). Thirdly, a rise in glucose disposal may result from ZnONPs' enhanced glycolysis (Hassan *et al.,* 2021).

Furthermore, zinc's direct involvement in the metabolism of proteins, carbs, and fats may be the source of ZnO NPs' antidiabetic actions. In the case of glucose metabolism, zinc is a cofactor of the important enzymes. It functions as both an inhibitor and an activator of fructose 1-6 diphosphate aldolase. ZnO NP treatment inhibits glycogenolysis and gluconeogenesis, two processes that are active when a person is fasting (Abd El-Rahman *et al.,* 2016). Because zinc signals insulin transduction, it often has effects similar to those of insulin. Furthermore, zinc has a crucial function in the production, storage, and secretion of insulin and has a proliferative and protective effect on the pancreatic islets.

Treatment with ZnO NPs may promote pancreatic cell regeneration and thereby raise insulin secretion. Our histology results further supported these effects, showing that ZnO NPs mostly restored the normal β cells while also regenerating the islets of Langerhans (Avila *et al.,* 2013).

Treatment with zinc may inhibit the intestinal α-glucosidase enzyme, which would decrease the absorption of glucose. Zinc also enhances the uptake of glucose in the liver, where it is subsequently stored (glycogenesis) (Amiri *et al.,* 2018). Zinc has a role in the GLUT's uptake of glucose as well as acting as an inhibitor of glucagon release, which lowers gluconeogenesis and glycogenolysis (Umrani and Paknikar, 2014).

According to the current study, ZnNPs can lower blood glucose levels in diabetics and preserve and antioxidant pancreatic cells, which enhances lipid metabolism and prevents consequences from diabetes (Samir *et al.,* 2022).

As a metabolic center, the liver plays a key role in regulating the body's normal glucose levels by stimulating and inhibiting hepatic glucose production. Since there is a link between altered hepatic physiology and diabetes, the liver gains particular significance because this equilibrium is frequently upset in diabetes (Al-Quraishy *et al.,* 2015).

The current study's results are consistent with those of Rezaei-Kelishadi *et al.* (2017), who discovered that the primary cause of the increases in ALT and AST activities in the serum of diabetic rats may be the liver cytosol's leakage of these enzymes into the bloodstream as a result of hepatic injury-associated diabetes mellitus. The pathophysiology of diabetes mellitus-induced hepatic inflammation is most likely another cause of the drop in blood albumin levels.

According to the findings of the current study by Gadoa *et al.* (2022), the diabetic group's serum levels of insulin and superoxide dismutase (SOD) were lower than those of the control group, while those of serum glucose, malondialdehyde, alanine aminotransferase (ALT), and aspartate aminotransferase (AST) were higher. These particular parameters were set aside for the ZnO NP treatment groups. This investigation shown that ZnO NPs improved liver function enzymes, blood glucose levels, and antioxidant status.

Our findings are in line with those of Ahmed *et al.* (2020), who found that administering ZnO NPs to diabetic groups caused a dose-dependent drop in ALT and AST levels.

The current study discovered a considerable rise in the mean values of AST and ALT in T2DM participants compared to healthy non-diabetic subjects. Our findings were in line with those of research by Salman *et al.,* Ghimire *et al.*, and Mathur *et al.*, (2016) which showed that the mean of both of these enzymes in DM was found to be considerably higher than in the control.

Similar research by Ghimire *et al.* has shown that there was just a little rise in the mean ALP in DM when compared to the control group. Compared to liver damage, ALP is much higher in liver cholestasis. Insulin resistance and hepatosteatosis cause an increase in ALP in T2DM (Mathur *et al*., 2016).

The results corroborate a prior study's conclusion that the STZ therapy increased the serum levels of alanine aminotransferase and aspartate aminotransferase in rat serum as compared to untreated rats (Bae and Ahn, 2022).

The outcomes were consistent with those reported by Jha *et al.* (2021), who observed that patients with type 2 diabetes had noticeably higher levels of AST, ALT, ALP, and GGT than did healthy individuals. However, there was a noticeable drop in albumin and total protein.

According to Miyamoto and Amrein's (2017) account, increased hepatic endogenous glucose production is caused by elevated gluconeogenic enzyme activity. This can result in persistent hyperglycemia and may be caused by insufficient insulin in diabetics.

Thankfully, current developments in nanomaterials have opened up new avenues for diabetes diagnosis and treatment (Liu *et al.,* 2022).

The current study's findings are consistent with those of Hassan *et al.* (2021), who reported that ZnONP treatment restored liver function to levels that were typical.

This calls for the quick development of low-cost antidiabetic nanomedicines. Effective design and development of antidiabetic therapies and sensing devices have demonstrated a wonderful potential and drawn enormous attention from the scientific community with the introduction of nano-bio research. Specifically, the properties of nanoparticles would improve absorption, selectivity, bioavailability, and biocompatibility. Accordingly, nanomaterials or nanocarriers are the best option (Sharma *et al.,* 2023).

According to Avila *et al.* (2013), our histology findings reinforced the effects even more, since ZnO NPs mostly restored the normal β cells and rejuvenated the islets of Langerhans. After treatment, compared to diabetic group rats, the diabetic groups treated with ZnO NPs and chitosan showed a large increase in serum insulin levels and a significant decrease in blood sugar levels.

When comparing the chitosan and ZnONP treatment groups to the diabetic group, there was a substantial decrease in glycated hemoglobin. Alkaladi *et al.*, 2014 demonstrated a significant drop in blood sugar and a rise in insulin levels in diabetic rats treated with ZnO NPs, which is consistent with our findings.

This revealed those nanoparticles' strong anti-diabetic properties. It has been demonstrated that zinc (Zn) is a potent metal that enhances the hepatic glycogenesis process by acting on the insulin signaling system, hence promoting glucose use and metabolism. The current study's findings were consistent with a number of earlier investigations. ZO NPs have been shown by Umrani and Paknikar (2014) to have potent antidiabetic activity and to be able to raise blood glucose levels in STZ-diabetic rats. Based on these findings, the researchers concluded that ZO NPs increased insulin secretion and synthesis in diabetic rats.

Due to its ability to decrease hepatic gluconeogenesis and increase skeletal muscle glucose absorption and utility, chitosan may be able to relieve the symptoms of diabetic hyperglycemia. Researchers also pay close attention to how chitosan oligosaccharide (COS) lowers blood glucose levels. COS supplementation inhibits gluconeogenesis and lipid peroxidation in the liver, which may ameliorate aberrant glucose metabolism in diabetic rats. In diabetic rats, lipid buildup in the liver and adipose tissue was inhibited and chronic inflammation was improved by high and low molecular weight chitosan feeding, which effectively lowered insulin resistance. In diabetic rats, COS can lower insulin resistance but less effectively lowers hepatic lipids (Tzeng *et al.,* 2022).

Furthermore, because of its demonstrated biological benefits, including its anti-inflammatory, anti-allergic, anticoagulant, anti-cancer, antibacterial, anti-human immune deficiency virus, anti-hypertensive, anti-Alzheimer's, anti-diabetic, anti-obesity, and matrix metalloproteinases inhibitory activities, chitosan is a promising bioactive material (Bakshi *et al.,* 2020).

In recent decades, chitosan-based nanoparticles—also known as chitosan nanoparticles, ChNPs, or chitosan-based nanocomposites-have drawn a lot of attention as promising materials. ChNPs are excellent candidates to be nanocarriers. They can provide a regulated release by encapsulating medications and active ingredients and delivering them to a certain location within the body (Jafernik *et al.,* 2023).

Researchers have established a connection between zinc levels, diabetes risk, and pathogenesis mechanisms ever since early publications showed low zinc contents in the serum and pancreas of diabetes patients. In addition to being necessary for the manufacture, storage, and structural stability of insulin, zinc also guards against oxidative stress, which is a factor in diabetes mellitus and its consequences (Rutter *et al.,* 2016). Zinc oxide is a member of a class of metallic oxides that have the ability to oxidize both chemical substances and living things (Amiri *et al.,* 2018).

ZON has the potential to be an innovative agent for the oral administration of zinc, as demonstrated by Asani *et al.* (2016).

Compared to the STZ-diabetic group, the hepatic SOD content of the ZnONP-treated STZ-diabetic rats was considerably higher. This resulted from zinc's role as a functional component of vital

antioxidant enzymes like SOD. Their production is hampered by zinc deficiency, which raises oxidative stress (Toma *et al.,* 2013).

According to Ukperoro *et al.* (2010), zinc may either have both effects or boost the manufacture of GSH while lowering oxidative stress and causing less GSH breakdown. This offered a possible explanation for how DM progression could be accelerated by a zinc deficit.

The results of this study are consistent with those of Othman *et al.* (2020), who discovered that the pancreatic tissues of diabetic rats had significantly lower levels of GSH and antioxidant enzyme activities (SOD, CAT, etc.); this could be because of oxidative stress brought on by hyperglycemia. In the meantime, ZO NP treatment dramatically increased the GSH level and these enzymes' activity in diabetic rats.

As predicted, our findings demonstrated that the diabetic rats' SOD and catalase activity were decreased. This could potentially be the result of oxidative damage brought on by hyperglycemia. Treatment with ZO NPs raised catalase and SOD levels in the serum.

Chronic illnesses, such as diabetes mellitus, are caused by persistent oxidative stress (Kamal *et al.,* 2019). Continuously high blood sugar levels during diabetes cause the production of free radicals, especially reactive oxygen species (ROS) (Wang and Wang, 2017). According to our data, the elevated ROS levels associated with diabetes led to a substantial reduction in SOD in the STZ-diabetic group as compared to the normal control group.

The results are consistent with earlier studies showing that the data from this study showed increased oxidative stress in diabetic rats along with concurrent impairment in the antioxidant defense systems. This was indicated by a significant increase in the oxidative stress biomarker (MDA) and a decrease in free-radical neutralizing antioxidants, such as SOD. Conversely, in diabetic rats, ZnO NPs treatment markedly increased SOD activities and considerably decreased levels (Oztürk *et al.,* 2015).

5. Conclusion

In conclusion, zinc oxide nanoparticles influence the management of diabetes. ZnONPs have the potential to be used as anti-diabetic drugs since they rebuild the structure and function of the β cells. ZnONP supplementation may stop the progression of type 2 diabetes in people who are pre-diabetic.

Zinc oxide nanoparticles (ZnO NPs) have been shown to significantly reverse the damage that diabetes has caused to the pancreas. This has been validated by the biochemical normalization of blood glucose and serum insulin levels, as well as enhanced structure and ultrastructure. In test animals, ZnO NPs appeared to have some potential efficacy. Therefore, ZnO NPs are advised as anti-diabetic drugs. Before being utilized as a regular treatment, however, a number of clinical trials of varying sizes, doses, and durations are required for its administration to humans.

Acknowledgements

Authors are thankful to Head Department of biology and Head Department of pharmacology of king Abdulaziz university, Jeddah, for providing necessary facilities for experimental work.

References

Abd El-Rahman, N.S., S.M. Reda, and S.M. AlGhannam, 2016. Synthesis and characterization of nano-doped zinc oxide and its application as protective oxidative changes in the retina of diabetic rats. Journal of Diabetes & Metabolism., 7(7): 1–6.

Abdulmalek, S.A. and M. Balbaa, 2019. Synergistic effect of nano-selenium and metformin on type 2 diabetic rat model: diabetic complications alleviation through insulin sensitivity, oxidative mediators and inflammatory markers. PLoS One., 14(8): 220-779.

Afify, M., N. Samy, N.A. Hafez, A.S. Alazzouni, M. El sayed., H. El mezyen, and M. M. Kelany, 2019. Evaluation of Zinc-oxide Nanoparticles Effect on Treatment of Diabetes in Streptozotocin-induced Diabetic Rats. Egypt. J. Chem., 62(10): 1771 – 1783.

Ahmed, F., Q. Husain, M.O. Ansari, and G.G.H.A. Shadab, 2020. Antidiabetic and oxidative stress assessment of bio-enzymatically synthesized zinc oxide nanoformulation on streptozotocin-induced hyperglycemic mice. Appl. Nanosci., 10: 879-893.

Albarakaty, F.M., M.I. Alzaban, N.K. Alharbi, F.S. Bagrwan, A.R. Abd El-Aziz, and M. A. Mahmoud, 2023. Zinc oxide nanoparticles, biosynthesis, characterization and their potent photocatalytic degradation, and antioxidant activities. Journal of King Saud University-Science., 35(1): 102434.

Alizadeh, A.H.M., 2020. Diabetes Mellitus and Pancreas: An Overview. Journal of the Pancreas., 21(4): 72-73.

Aljabali, A., Y. Akkam, M. Al Zoubi, K. Al-Batayneh, B. Al-Trad, O. Abo Alrob, A. Alkilany, M. Benamara, and D. Evans, 2018. Synthesis of gold nanoparticles using leaf extract of *Ziziphus zizyphus* and their antimicrobial activity. Nanomaterials., 8(3): 174.

Alkaladi, A., M.A. Aaser, and A. Mohamed, 2014. AntidiabeticActivity of Zinc Oxide and Silver Nanoparticles on Streptozotocin- Induced Diabetic Rats. Int. J. Mol. Sci., 15: 2015- 2023.

Al-Quraishy, S., M.A. Dkhil, and A.E. Abdel Moneim, 2015. Antihyperglycemic activity of selenium nanoparticles in streptozotocin-induced diabetic rats. Int J Nanomedicine., 10: 6741–6756.

Amiri A., R.F. Dehkordi, M.S. Heidarnejad, and M. J. Dehkordi, 2018. Effect of the zinc oxide nanoparticles and thiamine for the management of diabetes in alloxan-induced mice: a stereological and biochemical study. Biol Trace Elem Res., 18(12): 258–264.

Asani, S.C., R.D. Umrani, and K.M. Paknikar, 2016. In vitro studies on the pleotropic antidiabetic effects of zinc oxide nanoparticles. Nanomedicine (Lond)., 11(13):1671-1687.

Avila, D.L., G.R.D. Araújo, M. Silva, P.H.D.A. Miranda, M.F. Diniz, M.L. Pedrosa, M.E. Silva, W.G.D. Lima, and D.C. Costa, 2013. Vildagliptin Ameliorates Oxidative Stress and Pancreatic Beta Cell Destruction in Type 1 Diabetic Rats. Archives of Medical Research., 44(3): 194–202.

Aziz, M.T.A., M.F. El-Asmar, A.M. Rezq, S.M. Mahfouz, M.A. Wassef, H.H. Fouad, H.H. Ahmed, and F.M. Taha, 2013. The effect of a novel curcumin derivative on pancreatic islet regeneration in experimental type-1 diabetes in rats (long term study). Diabetology & Metabolic Syndrome., 5(1): 75.

Bae, C.S. and T. Ahn, 2022. Albumin infusion ameliorates liver injury in streptozotocin-induced diabetic rats. Vet Med-Czech., 67: 245-256.

Bala, N., S. Saha, M. Chakraborty, M. Maiti, S. Das, R. Basu, and P. Nandy, 2015. Green synthesis of zinc oxide nanoparticles using *Hibiscus subdariffa* leaf extract: effect of temperature on synthesis, anti-bacterial activity and anti-diabetic activity. RSC Advances., 5: 4993–5003.

Bakshi, P.S., D. Selvakumar, K. Kadirvelu, and N.S. Kumar, 2020. Chitosan as an environment friendly biomaterial – a review on recent modifications and applications. International journal of biological macromolecules., 1072-1083.

Bennett, R.A. and A.E. Pegg, 1981. Alkylation of DNA in rat tissues following administration of streptozotocin. Can. Res., 41: 2786-2790.

Bowers, G.N. and R.B. Mccomb, 1966. A continuous spectrophotometric method for measuring the activity of serum alkaline phosphatase. Clinical chemistry., 12(2): 70-89.

Cao, S., Y. Deng, L. Zhang, and M. Aleahmad, 2022. Chitosan Nanoparticles, as Biological Macromolecule-Based Drug Delivery Systems to Improve the Healing Potential of Artificial Neural Guidance Channels: A Review. Int. J. Biol. Macromol., 20: 569-579.

Carmen, P., J. Gómez, and J.A. Cecili, 2020. Chitosan: A Natural Biopolymer with a Wide and Varied Range of Applications. Molecules., 1(25): 3981.

Carter, P., 1970. Ultramicroestimation of human serum albumin binding of the cationic dye 5,5'-dibromo-o-cresolsulfonphthalein. Microchem J., 15(4): 531-539.

Chaudhari, A.A., U.J. Tupe, A.V. Patil, and C.G. Dighavkar, 2022. Synthesis and Characterization of Zinc Oxide Nanoparticles Using Green Synthesis Method. International Journal of Creative Research Thoughts., 10: 301-308.

Dawn-Linsley, M., F.J. Ekinci, D. Ortiz, E. Rogers, and T.B. Shea, 2005. Monitoring thiobarbituric acid-reactive substances (TBARs) as an assay for oxidative damage in neuronal cultures and central nervous system. Journal of neuroscience methods., 141(2): 219-222.

Demissie, M.G., F.K. Sabir, G.D. Edossa, and B.A. Gonfa, 2020. Synthesis of Zinc Oxide Nanoparticles Using Leaf Extract of *Lippia adoensis* (Koseret) and Evaluation of Its Antibacterial Activity. Journal of Chemistry., 1–9.

Dimassi, S., N. Tabary, F. Chai, N. Blanchemain, and B. Martel, 2018. Sulfonated and sulfated Chitosan Derivatives for Biomedical Applications: A Review. Carbohydr. Polym., 202: 382–396.

Doumas, B., B. Perry, B. Jendrzejczak, and L. Davis, 1987. Measurement of direct bilirubin by use of bilirubin oxidase. Clinical chemistry., 33(8): 1349-1353.

Duru, K.C., E.G. Kovaleva, I.G. Danilova, P.V.D. Bijl, and A.V. Belousova, 2018. The potential beneficial role of isoflavones in type 2 diabetes mellitus. Nutr Res., 59: 1-15.

El-Gharbawy, R.M., A.M. Emara, and S.E.S. Abu-Risha, 2016. Zinc oxide nanoparticles and a standard antidiabetic drug restore the function and structure of beta cells in Type-2 diabetes. Biomedicine & Pharmacotherapy., 84: 810-820.

Elkomy, M.H., A.A. Ali, and H.M. Eid, 2022. Chitosan on the Surface of Nanoparticles for Enhanced Drug Delivery: A Comprehensive Review. J. Control. Release., 351: 923-940.

Endah, E.S., V. Saraswaty, D. Ratnaningrum, W. Kosasih, A. Ardiansyah, C. Risdian, P. Nugroho, E.S. Aji, and H Setiyanto, 2023. Phyto-assisted synthesis of zinc oxide nanoparticles using mango (Mangifera indica) fruit peel extract and their antibacterial activity. IOP Conf. Series: Earth and Environmental Science., 1201: 012081, 1-7.

Feldman, A.T. and D. Wolfe, 2014. Tissue processing and hematoxylin and eosin staining. Histopathology. Springer., 31-43.

Gadoa, Z.A., A.H. Moustafa, S.M. El Rayes, A.A. Arisha, and M.F. Mansour, 2022. Zinc Oxide Nanoparticles and Synthesized Pyrazolopyrimidine Alleviate Diabetic Effects in Rats Induced by Type II Diabetes. ACS Omega., 7(41): 36865–36872.

Ghimire, S., S. Shakya, J. Shakya, P. Acharya, and B. D. Pardhe, 2018. Abnormal Liver Parameters among Individuals with Type 2 Diabetes Mellitus Nepalese Population. Biochem Pharmacol (Los Angel)., 7: 243.

Gjorgjieva, M., G. Mithieux, and F. Rajas, 2019. Hepatic stress associated with pathologies characterized by disturbed glucose production. Cell Stress., 3(3): 86–99.

Guan, Z. and Q. Feng, 2022. Chitosan and chitooligosaccharide: The promising non-plant-derived prebiotics with multiple biological activities. Int. J. Mol. Sci., 23: 6761.

Günister, E., D. Pestreli, C.H. Ünlü, O. Atıcı, and N. Güngör, 2007. Synthesis and characterization of chitosan-MMT biocomposite systems. Carbohydrate Polymers., 67(3): 358–365.

Guo, W., L. Yi, B. Zhou, and M. Li, 2020. Chitosan modifies glycemic levels in people with metabolic syndrome and related disorders: Meta-analysis with trial sequential analysis. Nutr J., 19: 130.

Hasnain M.S. and A.K. Nayak, 2022. Chitosan as Mucoadhesive Polymer in Drug Delivery. In Chitosan in Drug Delivery. Academic Press: Cambridge., 225-246.

Hassan, R.M., M. Elsayed, T.E. Kholief, N.H.M. Hassanen, J.A. Gafer, and Y.A. Attia, 2021. Mitigating effect of single or combined administration of nanoparticles of zinc oxide, chromium oxide, and selenium on genotoxicity and metabolic insult in fructose/streptozotocin diabetic rat model. Environmental Science and Pollution Research., 28: 48517- 48534.

Hawrysz, Z. and A. Woźniacka, 2023. Zinc: an undervalued microelement in research and treatment. Adv Dermatol Allergol., (2): 208–214.

Heidari, F., S.M. Jafari, A.M. Ziaiifar, and N. Anton, 2023. Surface modification of silica nanoparticles by chitosan for stabilization of water-in-oil Pickering emulsions. Carbohydrate Polymer Technologies and Applications., 6: 100381.

Henry, J., 2001. Clinical Diagnosis and Management by Laboratory Methods. W. B. Saunders Company, Twentieth Philadelphia, PA., 47(12): 2188-2189.

Hu, Y., H. Zhang, L. Dong, M. Xu, L. Zhang, W. Ding, and P. Wei, 2019. Enhancing tumor chemotherapy and overcoming drug resistance through autophagy mediated intracellular dissolution of zinc oxide nanoparticles. Nanoscale., 11: 11789–11807.

Huang D.Q., N. Noureddin, V. Ajmera, M. Amangurbanova, R. Bettencourt, E. Truong, T. Gidener, H. Siddiqi, A. M. Majzoub, T. Nayfeh, N. Tamaki, N. Izumi, M. Yoneda, A. Nakajima, R. Idilman, M. Gumussoy, D.K. Oz, A. Erden, A.M. Allen, M. Noureddin, and R. Loomba, 2023. Type 2 diabetes, hepatic decompensation, and hepatocellular carcinoma in patients with non-alcoholic fatty liver disease: an individual participant-level data meta-analysis. Lancet Gastroenterol Hepatol., 8: 829-36.

Jafernik, K., A. Ładniak, E. Blicharska, K. Czarnek, H. Ekiert, A.E. Wiacek, and A. Szopa, 2023. Chitosan-Based Nanoparticles as Effective Drug Delivery Systems—A review. Molecules., 28: 1963.

Javed, R., F. Rais, H. Fatima, I.U. Haq, M. Kaleem, S.S. Naz, and Q. Ao, 2020. Chitosan encapsulated ZnO nanocomposites: Fabrication, characterization, and functionalization of bio-dental approaches. Materials Science and Engineering C., 116: 1-19.

Jendrassik, L. and P. Grof, 1938. Colorimetric method of determination of bilirubin. Biochem Z., 297(81): 81-82.

Jha, S.K., N.K. Yadav, and S. Rizal, 2021. Prevalence of elevated liver enzymes and its association with type 2 diabetes: A Descriptive Cross-Sectional Study among Nepalese Adults from Biratnagar, Nepal. Asian Journal of Medical Sciences., 12(6): 1-6.

Joseph, J., P. Badrinath, G.S. Basran, and S.A. Sahn, 2001. Is the pleural fluid transudate or exudate? A revisit of the diagnostic criteria. Thorax., 56(11): 867-70.

Kamal, A., U. Haroon, H. Manghwer, K.H. Alamer, I.M. Alsudays, A.T. Althobaiti, A. Iqbal, M. Akbar, M. Anar, Farhana, M. Anar, M. Nazish, H. J. Chaudhary, and M.F.H. Munis, 2022. Biological Applications of Ball-Milled Synthesized Biochar-Zinc Oxide Nanocomposite Using Zea mays L. Molecules., 27(16): 1-20.

Kamal, M., M. Khairy, N. ELSadek, and M. Hussein, 2019. Therapeutic efficacy of zinc oxide nanoparticles in diabetic rats. Slov. Vet. Res., 56: 187-194.

Keerthana, S. and A. Kumar, 2020. Potential risks and benefits of zinc oxide nanoparticles: a systematic review. Critical Reviews in Toxicology., 1-27.

Kim, S.Y. and D.H. Park, 2009. Preparation of ZnO nanopowders by thermal plasma and characterization of photo-catalytic property. Appl. Surf. Sci., 255(10): 5363-5367.

Kingsley, G.R., 1942. The direct biuret method for the determination of serum proteins as applied to photoelectric and visual colorimetry. Journal of Laboratory and Clinical Medicine., 27: 840-845.

Kliszczewska, E., 2020. Gluatathion peroxidase (GPx) and superoxide dismutase (SOD) activity in patients with diabetes mellitus type 2 infected with Epstein-Barr virus. Plos One., 15(3): 1-10.

Kumar, M., S. Dandapat, M.P. Sinha, A. Kumar, and B.S. Raipat, 2017 Different blood collection methods from rats: A review. Balneo Reseaech journal., 8(2): 46-50.

Ładniak, A., M. Jurak, M. Palusińska-Szysz, and A.E. Wiącek, 2022. The Influence of Polysaccharides/TiO2 on the Model Membranes of Dipalmitoylphosphatidylglycerol and Bacterial Lipids. Molecules., 27(2): 343.

Lai, H., Y. Liu, G. Huang, Y. Chen, Y. Song, Y. Ma, Y. Pengfei, 2021. Fabrication and antibacterial evaluation of peppermint oil-loaded composite microcapsules by chitosan-decorated silica nanoparticles stabilized Pickering emulsion templating International Journal of Biological Macromolecules., 183: 2314-2325.

Liou, T. H., S. Y. Wang, Y. T. Lin, and S. Yang, 2022. Sustainable Utilization of Rice Husk Waste for Preparation of Ordered Nanostructured Mesoporous Silica and Mesoporous Carbon: Characterization and Adsorption Performance. Colloids Surf. A Physicochem. Eng. Asp., 636: 128150.

Liu, Y., S. Zeng, W. Ji, H. Yao, L. Lin, H. Cui, H.A. Santos, and G. Pan, 2021. Emerging Theranostic Nanomaterials in Diabetes and ItsComplications. Adv. Sci., 9: 1-54.

Louderback, A. L. and E. Shanbrom, 1968. Lactic dehydrogenase isoenzyme electrophoresis. JAMA., 205(5): 294-295.

Malatesta, M., 2021. Transmission Electron Microscopy as a Powerful Tool to Investigate the Interaction of Nanoparticles with Subcellular Structures. Int J Mol Sci., 22(23): 12789.

Maret, W., 2017. Zinc in pancreatic islet biology, insulin sensitivity, and diabetes. Preventive Nutrition and Food Science., 22(1): 1-8.

Mathur, S., D.K. Mehta, S. Kapoor, and S. Yadav, 2016. Liver Function in Type-2 Diabetes Mellitus Patients. Int J Sci Stud., 3(10): 43-47.

Miao, L., B. Shi, N. Stanislaw, C. Mu, and W.H. Herman, 2017. Facile synthesis of hierarchical ZnO microstructures with enhanced photocatalalytic activity. Materials Sience-Poland., 35(1): 45-49.

Miyamoto, T. and H. Amrein, 2017. Gluconeogenesis: An ancient biochemical pathway with a new twist. Taylor & Francis., 11(3): 218-223.

Mohamed, J., A.H. Nazratun NaBzah, A.H. Zariyantey, and S.B. Budin, 2016. Mechanisms of diabetes-induced liver damage: the role of oxidative stress and inAammation. Sultan Qaboos University Medical Journal., 16(2): 132-141.

Mona, H., H. Saba, V. Kambiz, and V. Hojat, 2018. Green synthesis, antibacterial, antioxidant and cytotoxic effect of gold nanoparticles using *Pistacia atlantica* extract. Journal of Taiwan Institute of Chemical Engineers., 1:1–10.

Nandanwar, P.M., D. Saravanan, P. Bakshe, and R. M. Jugade, 2022. Chitosan entrapped microporous activated carbon composite as a supersorbent for remazol brilliant blue R. Materials Advances., 3(13): 5488-5496.

Naser, M., M.M. Nasr, and L.H. Shehata, 2021. Nanotechnology in Diagnosis and Treatment of Diabetes Mellitus. International Journal of Progressive Sciences and Technologies., 24(1): 586-596.

Nozipho, P., Gamedze, M.N. Doctor, Mthiyane, M. Sydney, S. Moganavelli, D.C. Onwudiwe, 2023. Biosynthesis of ZnO Nanoparticles Using the Aqueous Extract of *Mucuna pruriens* (utilis): Structural Characterization, and the Anticancer and Antioxidant Activities. Chemistry Africa., 1-10.

Oltulu, F., A. Buhur, Ç. Gürel, G.C. Kuşçu, M. Dağdeviren, N.Ü.K. Yavaşoğlu, T. Köse, and A. Yavaşoğlu, 2019. Mid-dose losartan mitigates diabetes-induced hepatic damage by regulating iNOS, eNOS, VEGF, and NF-BB expressions. Turkish Journal of Medical Sciences., 49(5): 1582–1589.

Ong, C.B., L.Y. Ng, and A.W. Mohammad, 2018. A review of ZnO nanoparticles as solar photocatalysts: Synthesis, mechanisms and applications. Renew. Sustain. Energy Rev., 81(1): 536-551.

Othman, M.S., M.M. Hafez, and A.E. Abdel Moneim, 2020. The Potential Role of Zinc Oxide Nanoparticles in MicroRNAs Dysregulation in STZ-Induced Type 2 Diabetes in Rats". Biological Trace Element Research., 197: 606-618.

Oztürk, Z., T. Gurpinar, K. Vura, S. Boyacıoglu, M. Korkmaz, and A. Var, 2015. Effects of selenium on endothelial dysfunction andmetabolic profile in low dose streptozotocin induced diabetic rats fed a high fat diet. Biotech Histochem., 90: 506-515.

Padhi, S., A. Kumar, and A. Behera, 2020. Biomedicine and Pharmacotherapy Type II diabetes mellitus: a review on recent drug based therapeutics. Biomedicine and Pharmacotherapy., 131: 110708.

Phuong, D.T.M., N.T.T. Thao, and N.X. Loc, 2023. Preparing Shrimp Shell-Derived Chitosan with Rice Husk-Derived Biochar for Efficient Safranin O Removal from Aqueous Solution. Journal of Ecological Engineering., 24(1): 248-259.

Pokhrel, S., R. Lach, H.H. Le, A. Wutzler, W. Grellmann, H. Radusch, P.R. Dhakal, A. Esposito, S. Henning, N.P. Yadav, M.J. Saiter, G. Heinrich, and R. Adhikari**,** 2016. Fabrication and Characterization of Completely Biodegradable Copolyester–Chitosan Blends:I. Spectroscopic and Thermal Characterization Macromol. Symp., 366: 23–34.

Priyanka, D.N., K.V. Harish Prashanth, and R.N. Tharanathan, 2022. A review on potential anti-diabetic mechanisms of chitosan and its derivatives. Carbohydrate Polymer Technologies and Applications., 1-10.

Raj, R., 1977. Effect of incubation with Mg2+ on the measurement of alkaline phosphatase activity. Clinical chemistry., 23(10): 1903-1911.

Rezaei-Kelishadi, M., A. Ghasemi, N.N. Abdolyosefi, S. Zamani-Doabi, M. Ramezani, S. Changizi-Ashtiyani, and A. Rahimi, 2017. Effects of selenium nanoparticles on kidney and liver functional disorders in streptozotocin-induced diabetic rats. J Physiol Pharmacol., 21:155–162

Rodrigues, I., G. Punaro, D. Lima, T.C.D. Bessa, M. Mouro, A. Bertolini, A. Rodrigues, R. Serralha, and E.M.S. Higa, 2020. Oxidative stress in the heart of rats with diabetic nephropathy treated with esculin. Free Radical Biology and Medicine., 159: 73-74.

Rutter, G.A., P. Chabosseau, E.A. Bellomo, W. Maret, R.K. Mitchell, D.J. Hodson, A. Solomou, and M. Hu, 2016. Intracellular zinc in insulin secretion and action: a determinant of diabetes risk. Proc Nutr Soc., 75(1): 61–72.

Salman, M.I., R.M. Rashied, and H.S. Hamad, 2020. Study of liver function tests in diabetes type-2 patients in Ramadi city, Iraq, Western Iraq, Ann Trop Med and Public Health., 23(18): SP231824.

Samir, D., B. Ouissam, and D. Anfal, 2022. Antioxidant and Antidiabetic Effect of Biosynthesis Zinc Nanoparticles by Using Polyherbal Aqueous Extract in Wistar Rats. J. Biochem. Technol., 13(1): 72-80.

Shaban, E.E., M. E. Abd El-Aziz, K.S. Ibrahim, S.M. Nasr, H.M. Desouky, and H.F.H. Elbakry, 2022. Effect of zinc oxide nanoparticles on diabetes development and complications in diabetic rats compared to conventional zinc sulfate and metformin. Biocatalysis and Agricultural Biotechnology., 46: 102538.

Sharma, R., S.J. Borah, Bhawna, S. Kumar, A. Gupta, V. Kumari, R. Kumar, K.K. Dubeyg, and V. Kumar, 2023. Emerging trends in nano-based antidiabetic therapeutics: a path to effective diabetes management. Mater. Adv., 4: 3091-3113.

Shaw, L.M., J.H. Strømme, J.L. London, and L. Theodorsen, 1983. IFCC methods for the determination of enzymes part 4. IFCC method for gamma-glutamyl transferase [(gamma-glutamy)-peptide; amino acid gamma-glutamyl transferase, EC 2.3.2.2]. clinica chimica acta., 21(10): 633-46.

Sumaila, A., M.M. Ndamitso, Y.A. Iyaka, A.S. Abdulkareem, J. O. Tijani, and M.O. Idris, 2020. Extraction and Characterization of Chitosan from Crab Shells: Kinetic and Thermodynamic Studies of Arsenic and Copper Adsorption from Electroplating Wastewater. Iraqi Journal of Science., 61(9): 2156-2171.

Tabatabaie-Malazy, O., M. Khodaeian, F. Bitarafan, B. Larijani, and M.M. Amoli, 2017. Polymorphisms of Antioxidant Genes as a Target for Diabetes Management. Int J Mol Cell Med., 6(3): 135–147.

Taziwa, R., E. Meyer, D. Katwire, and L. Ntozakhe, 2017. Influence of carbon modification on the morphological, structural, and optical properties of zinc oxide nanoparticles synthesized by pneumatic spray pyrolysis technique. Journal of Nanomaterials., 1-11.

Tietz, F., V. Haanappel, A. Mai, J. Mertens, and D. Stöver, 2006. Performance of LSCF cathodes in cell tests. Journal of Power Sources., 156(1): 20-22.

Toma, A., E. Makonnen, and G. Yimer, 2013. Role of zinc in diabetes mellitus, oxidative stress and other human healthy. Am. J. Res. Commun., 1(11): 411–426.

Tzeng, H.P., S.H. Liu, and M.T. Chiang, 2022. Antidiabetic Properties of Chitosan and Its Derivatives. Mar. Drugs., 20: 784.

Ukperoro, J.U., N. Offiah, T. Idris, and D. Awogoke, 2010. Antioxidant effect of zinc, selenium and their combination on the liver and kidney of alloxan-induced diabetes in rats. Mediterr J Nutr Metab., 3(1): 25-30.

Umrani, D.R. and K.M. Paknikar, 2014. Zinc oxide nanoparticles show antidiabetic activity in streptozotocin-induced Types 1 and 2 diabetic rats. Nanomedicine., 9(1): 89-104.

Vijayakumar, S., B. Vaseeharan, B. Malaikozhundan, and M. Shobiya,Laurus 2016. Nobilis Leaf Extract Mediated Green Synthesis of ZnO Nanoparticles: Characterization and Biomedical Applications. Biomed. Pharmacother., 84: 1213-1222.

Vijayakumar, S., P. Arulmozhi, N. Kumar, B. Sakthivel, S. Prathip Kumar, P.K. Praseetha, and L. Acalypha Fruticosa, 2020. Leaf Extract Mediated Synthesis of ZnO Nanoparticles: Characterization and Antimicrobial Activities. Mater. Today: Proc., 23: 73-80.

Vijayakumar, S., S. Mahadevan, P. Arulmozhi, S. Sriram, and P.K. Praseetha, 2018. Green Synthesis of Zinc Oxide Nanoparticles Using Atalantia Monophylla Leaf Extracts: Characterization and Antimicrobial Analysis. Mater. Sci. Semicond. Process., 82: 39-45.

Walunj, P., A. Roy, V. Jadhav, P. Athare, A. Dhaygude, J. Aher, J.S. Algethami, D. Lokhande, M.S. Alqahtani, A. Bhagare, S. Alghamdi, L.B. Eltayeb, I.S. Al-Moraya, K.K. Yadav, Y. Ahn, and B.H. Jeon, 2023. Polyol-mediated zinc oxide nanoparticles using the refluxing method as an efficient photocatalytic and antimicrobial agent. Front. Bioeng. Biotechnol., 11: 1177981.

Wang, J. and H. Wang, 2017. Oxidative stress in pancreatic beta cell regeneration. Oxid. Med. Cell. Longevity., 1-9.

Wang, J., L. Wang, L. Long, Q. Tao, F. Xu, and F. Luo, 2019. Solitary renal metastasis from squamous cell carcinoma of the lung: a case report. Medicine (Baltimore)., 98(5): 1-3.

Wang, W., Q. Meng, Q. Li, J. Liu, M. Zhou, Z. Jin, and K. Zhao, 2020. Chitosan Derivatives and Their Application in Biomedicine. Int. J. Mol. Sci., 21(487): 1-26.

Ways, T.M.M., W.M. Lau, and V.V. Khutoryanskiy, 2018. Chitosan and Its Derivatives for Application in Mucoadhesive Drug Delivery Systems. Polymers., 10 (3): 267.

Xiong, X. and X. Li, 2023. Type 2 diabetes originated from non-alcoholic fatty liver disease. Life Metabolism., 2(1): 1-3.

Yagi, K., 1998. Simple assay for the level of total lipid peroxides in serum or plasma, Free radical and antioxidant protocols. Methods Mol Biol., 108: 101-106.

Yedurkar, S., C. Maurya, and P. Mahanwar, 2016. Biosynthesis of Zinc Oxide nanoparticles using *Ixora Coccinea* Leaf Extract-A green approach. Open Journal of Synthesis Theory and Applications., 5: 1-14.

Zafar, M., S. Naqvi, M. Ahmed, and Z.A. Kaimkhani, 2009. Altered kidney morphology and enzymes in streptozotocin-induced diabetic rats. Int. J. Morphol., 27(3): 783-790.

Zewde, D. and B. Geremew, 2022. Biosynthesis of ZnO nanoparticles using Hagenia abyssinica leaf extracts; their photocatalytic and antibacterial activities. Environmental pollutants and bioavailability., 34(1) 224-235.

Zhang, S., H. Gao, and G. Bao, 2015. Physical Principles of Nanoparticle Cellular Endocytosis. ACS Nano., 9(9): 8655-8671.

Zhou, J.C., J.J. Zhang, W. Zhang, Z.Y. Ke, and B. Zhang, 2017. Efficacy of chitosan dressing on endoscopic sinus surgery: a systematic review and meta-analysis. Eur Arch Otorhinolaryngol., 274(9): 3269-3274.

Zhou, X.Q., Z. Hayat, D.D. Zhang, M.Y. Li, S. Hu, Q. Wu, Y.F. Cao, and Y. Yuan, 2023. Zinc Oxide Nanoparticles: Synthesis, Characterization, Modification, and Applications in Food and Agriculture. Processes., 11: 1193.